Reliability Modeling Using Weibull Distribution in Partially Accelerated Life Tests with Unified Hybrid Censoring: White Organic LEDs and Micro-Droplet Applications

Ohud A. Alqasem[1], Mazen Nassar[2,*], Maysaa Elmahi Abd Elwahab[1] and Ahmed Elshahhat[3]

[1] Department of Mathematical Sciences, College of Science, Princess Nourah bint Abdulrahman University, Riyadh, 11671, Saudi Arabia

[2] Department of Statistics, Faculty of Science, King Abdulaziz University, Jeddah, 21589, Saudi Arabia

[3] Faculty of Technology and Development, Zagazig University, Zagazig, 44519, Egypt

INFORMATION

Keywords:
Weibull distribution
accelerated life tests
unified hybrid censoring
Bayesian estimation
reliability estimation

DOI: 10.23967/j.rimni.2025.10.71073

SCIPEDIA Revista Internacional de Métodos Numéricos para Cálculo y Diseño en Ingeniería

Revista Internacional Métodos numéricos para cálculo y diseño en ingeniería RIMNI

In cooperation with CIMNE

Reliability Modeling Using Weibull Distribution in Partially Accelerated Life Tests with Unified Hybrid Censoring: White Organic LEDs and Micro-Droplet Applications

Ohud A. Alqasem[1], **Mazen Nassar**[2,*], **Maysaa Elmahi Abd Elwahab**[1] **and Ahmed Elshahhat**[3]

[1]Department of Mathematical Sciences, College of Science, Princess Nourah bint Abdulrahman University, Riyadh, 11671, Saudi Arabia

[2]Department of Statistics, Faculty of Science, King Abdulaziz University, Jeddah, 21589, Saudi Arabia

[3]Faculty of Technology and Development, Zagazig University, Zagazig, 44519, Egypt

ABSTRACT

Accelerated life testing has become essential in modern reliability assessment, particularly for high-reliability products where traditional testing is often impractical due to time constraints. This study introduces a comprehensive framework for reliability analysis using Weibull-based partially accelerated life tests under a unified hybrid censoring scheme. Assuming lifetimes follow a Weibull distribution, we provide both classical and Bayesian estimation procedures to estimate core quantities, shape, scale, and the acceleration factor, alongside reliability metrics at normal operating conditions. The inferential framework encompasses point estimation along with uncertainty quantification, using both approximate confidence intervals and Bayesian credible intervals derived from Markov Chain Monte Carlo methods. A comprehensive Monte Carlo simulation study evaluates the performance of various methods in terms of mean squared error, interval coverage, and average interval width across a range of censoring patterns. The results provide actionable insights and practical recommendations for selecting appropriate methods and designing future studies under different censoring scenarios. The proposed methodology is further illustrated through two real-world case studies: the reliability of white organic light-emitting diodes and the lifetime of micro-droplets in ambient environments. These examples highlight the method's flexibility and practical relevance in both engineering and biomedical reliability applications.

OPEN ACCESS

Received: 31/07/2025

Accepted: 10/09/2025

Published: 23/01/2026

DOI
10.23967/j.rimni.2025.10.71073

Keywords:
Weibull distribution
accelerated life tests
unified hybrid censoring
Bayesian estimation
reliability estimation

1 Introduction

Nowadays, rapid technological progress and severe competition among manufacturers have made it increasingly expected to produce highly reliable products. However, examining the reliability of such products presents challenges, as it often takes a significant amount of time to observe failures, which is a critical step in life testing to evaluate product reliability. To address this issue, researchers frequently turn to accelerated life tests (ALTs) as an efficient method for evaluating the lifetimes of these highly

*Correspondence: Mazen Nassar (mmohamad3@kau.edu.sa or mezo10011@gmail.com).

reliable products. In ALTs, products are subjected to higher-than-normal stress conditions, such as elevated temperatures, increased voltage, or additional weight, to induce failures more quickly. By analyzing failure data obtained under these extreme stress conditions, researchers can then extrapolate and make informed predictions about the product's reliability under normal operating circumstances. There are various methods for conducting ALTs, but the two most commonly employed approaches are the constant-stress and step-stress ALTs.

In constant-stress ALTs, each test unit is continuously exposed to a fixed level of stress until all units have failed. On the other hand, in step-stress ALTs, the stress levels are incrementally increased at specific time intervals or after a pre-set number of failures has been observed. For further studies on constant-stress ALTs, one may refer to Watkins and John [1], Fan and Yu [2], El-Din et al. [3], Abd El-Raheem [4], Kumar et al. [5], Wu et al. [6], Mohamed et al. [7]. In contrast, for more comprehensive details regarding step-stress ALTs, see Tang et al. [8], Fard and Li [9], Han and Ng [10], Amleh and Raqab [11], and Kateri and Nikolov [12]. To evaluate a product's reliability under normal usage conditions employing data collected from ALTs, it is crucial to understand the life-stress model. This model establishes the relationship between a product's lifetime and the stress levels it is subjected to. However, life-stress models are not always predefined or assumed to be known. In such cases, partially accelerated life tests (PALTs) can serve as an effective strategy to assess reliability under normal operating conditions. Among the various types of PALTs, this research focuses on constant-stress PALT (CSPALT). In CSPALT, each item is tested exclusively under either normal or accelerated conditions, simplifying the analysis by avoiding the necessity of investigating the determination of stress models. Many authors considered the CSPALTs in their analysis, see for example. Hassan et al. [13], Nassr and Elharoun [14], Hassan et al. [15], Alomani et al. [16], Fayomi et al. [17], and Yao and Gui [18], among others.

Experimenters frequently face challenges in collecting complete lifetime data due to participant withdrawal, study time limits, or intentional removal of units in industrial experiments to save time and costs. Such scenarios result in incomplete data, known as censored data, which is common in life-testing, reliability studies, and survival analysis. To address this, researchers employ censoring schemes like Type-I and Type-II censoring. In Type-I censoring, the study runs until a fixed time T, with the number of failures being random. In Type-II censoring, a fixed number of failures $m \leq n$ are observed, with the endpoint being random, where n is the sample size, see El Gazar et al. [19]. Extensive research exists on statistical inference under these plans, as seen in Sirvanci and Yang [20], Abdel-Hamid and AL-Hussaini [21], and Ramzan et al. [22]. Suppose that $X_{1:n}, X_{2:n}, \ldots, X_{n:n}$ refer to the ordered failure times of units. Epstein [23] proposed Type-I hybrid censoring (HC) plan, where the test concludes at $\min\{X_{m:n}, T\}$, ensuring the experiment does not exceed a pre-specified time T. Later, Childs et al. [24] introduced Type-II HC scheme, in which the test ends at $\max\{X_{m:n}, T\}$, guaranteeing a fixed number of failures while potentially extending the testing duration. However, Type-I HC plan risks few failures, while Type-II HC plan may extend testing duration.

Chandrasekar et al. [25] improved these schemes with two generalized HC schemes. In the generalized Type-I HC plan, integers $k, m \in \{1, 2, \ldots, n\}$ with $k < m$ and a fixed time $T \in (0, \infty)$ are predefined. The experiment concludes at $\min\{X_{m:n}, T\}$ if the k-th failure occurs before T, or at $X_{k:n}$ otherwise, ensuring at least k failures. In the generalized Type-II HC plan, m and two fixed times $T_1, T_2 \in (0, \infty)$ with $T_1 < T_2$ are specified. The experiment terminates at T_1 if the m-th failure occurs before T_1, at $X_{m:n}$ if it occurs between T_1 and T_2, or at T_2, otherwise, ensuring the experiment is completed by T_2. However, certain limitations remain: the generalized Type-I HC plan cannot ensure the occurrence of m failures due to the predetermined time point T, while the generalized Type-II HC plan faces the risk of observing very few or even no failures. See for more details, Mahmoud and

Ghazal [26], and Alharthi and Almulhim [27]. To address the limitations inherent in both generalized Type-I and generalized Type-II hybrid censoring plans, Balakrishnan et al. [28] proposed the so-called unified hybrid censoring (UHC) scheme. This scheme will be discussed in the subsequent section in the context of CSPALTs.

Another critical consideration when analyzing lifetime data is the selection of an appropriate lifetime model. The Weibull distribution is one of the most commonly utilized lifetime models. Its prevalence in reliability and survival analysis can be attributed to its inherent flexibility and straightforward formulation. The Weibull distribution is capable of modeling positively skewed data with constant, increasing, and decreasing hazard rate functions (HRFs). Its versatility has led to extensive applications across various fields, including reliability engineering, hydrology, and communication systems. Given its adaptability and widespread acceptance, numerous researchers have incorporated the Weibull distribution into their studies, including, but not limited to, the work of Kundu and Gupta [29], Teimouri et al. [30], Starling et al. [31], Ramos et al. [32], and Nassar and Elshahhat [33], and Bahram et al. [34] among others. For further details on extensions of the Weibull distribution, readers may refer to Abouelmagd et al. [35], Elbatal et al. [36], Alyami et al. [37], and Noori et al. [38]. When the lifetime of a component, represented by the random variable X, is modeled by the Weibull distribution under normal operating conditions, its probability density function (PDF) is given by

$$f_1(x;\mu,\theta) = \mu\theta x^{\theta-1} e^{-\mu x^{\theta}}, x > 0, \mu, \theta > 0, \tag{1}$$

where μ and θ are the scale and shape parameters, respectively. The cumulative distribution function related to the random variable X is as follows

$$F_1(x;\mu,\theta) = 1 - e^{-\mu x^{\theta}}. \tag{2}$$

The reliability function (RF) and HRF of the Weibull distribution at normal operating conditions can be expressed, respectively, as

$$R_1(x;\mu,\theta) = e^{-\mu x^{\theta}} \quad \text{and} \quad H_1(x;\mu,\theta) = \mu\theta x^{\theta-1}. \tag{3}$$

The UHC plan is usefuel in concluding life-testing experiments, often resulting in a higher number of observable failures compared to generalized Type-I and Type-II HC schemes. However, its potential to improve statistical inference remains underexplored, particularly in the context of CSPALTs. Although some studies, such as those by Lone et al. [39], Alrashidi et al. [40], and Rabie and Abd-Elrahman [41], have applied the UHC scheme to estimate parameters of lifetime distributions under CSPALTs, they have overlooked crucial aspects of reliability analysis. Specifically, these studies have not addressed the estimation of key reliability metrics, such as the RF and HRF, under normal operating conditions which is the central objective in CSPALT-based reliability analysis. In addition, despite the widespread adoption of the Weibull distribution in reliability modeling, no studies within the UHC framework have tackled the challenges of estimating its parameters or associated reliability characteristics in the presence of CSPALTs. Addressing these limitations would significantly enhance the utility of the UHC plan in the context of CSPALTs in both theoretical results and real-world reliability applications. The primary objective of this study is to investigate the classical and Bayesian estimations of the Weibull distribution under the UHC plan in the context of CSPALTs. The estimations encompass the parameters of the Weibull distribution, the acceleration factor, as well as the RF and HRF under normal operating conditions, from both point and interval estimation perspectives. From the classical standpoint, the maximum likelihood method is employed to derive point estimates and approximate confidence intervals (ACIs). For the Bayesian approach, estimations are acquired using the squared error loss function, with Markov Chain Monte Carlo

(MCMC) procedures utilized for posterior inference. Simulation studies are performed to evaluate the effectiveness of the proposed estimation methods under various experimental scenarios. Additionally, the practical applicability of the methodologies is demonstrated through two real-world applications, which not only validate the proposed approaches but also assess the adequacy of the used model in real-life applications.

The remainder of this article is organized as follows: Section 2 provides a detailed description of the UHC plan within the framework of CSPALTs. In Section 3, we present the maximum likelihood estimators (MLEs) along with the ACIs for the model parameters, RF, and HRF under normal operating conditions. Section 4 focuses on Bayesian estimations, including point estimates and Bayes credible intervals (BCIs). The design and results of the simulation study are summarized in Section 5. Section 6 applies the proposed methodologies to two real-world examples, demonstrating their practical utility. Finally, several concluding observations are presented in Section 7.

2 Model Description and Test Methodology

Suppose we have a total of n test units. These units are split into two groups: the first group contains n_1 units, which are randomly chosen from the n test units and operated under normal operating conditions. The second group consists of the remaining $n_2 = n - n_1$ units, which are subjected to accelerated conditions. For each test group, the units are tested under the UHC plan with m_{k1}, m_{k2} $(m_{k1} < m_{k2}, k = 1, 2)$ and two thresholds $T_{k1} < T_{k2} \in (0, \infty)$. Accordingly, the UHC sampling plan in the context of CSPALT proceeds as follows:

1. If $X_{m_{k1}:n_k} < T_{k1}$, conclude the test at $\min\{\max(X_{m_{k2}:n}, T_{k1}), T_{k2}\}$.
2. If $T_{k1} < X_{m_{k1}:n_k} < T_{k2}$, end the test at $\min(X_{m_{k2}:n_k}, T_{k2})$.
3. If $X_{m_{k1}:n_k} > T_{k2}$, stop the test at $X_{m_{k1}:n_k}$.

It is clear to see that there are different scenarios under which the test may be terminated. Let $\tau_k, k = 1, 2$, denote the ending point. In this case, one of the following six possible observational scenarios can be observed:

- Case 1: $0 < X_{m_{k1}:n_k} < X_{m_{k2}:n_k} < T_{k1} < T_{k2}$, with termination point $\tau_k = T_{k1}$.
- Case 2: $0 < X_{m_{k1}:n_k} < T_{k1} < X_{m_{k2}:n_k} < T_{k2}$, with termination point $\tau_k = X_{m_{k2}:n_k}$.
- Case 3: $0 < X_{m_{k1}:n_k} < T_{k1} < T_{k2} < X_{m_{k2}:n_k}$, with termination point $\tau_k = T_{k2}$.
- Case 4: $0 < T_{k1} < X_{m_{k1}:n_k} < X_{m_{k2}:n_k} < T_{k2}$, with termination point $\tau_k = X_{m_{k2}:n_k}$.
- Case 5: $0 < T_{k1} < X_{m_{k1}:n_k} < T_{k2} < X_{m_{k2}:n_k}$, with termination point $\tau_k = T_{k2}$.
- Case 6: $0 < T_{k1} < T_{k2} < X_{m_{k1}:n_k} < X_{m_{k2}:n_k}$, with termination point $\tau_k = X_{m_{k1}:n_k}$.

In this case, we have two UHC samples under CSPALTs, denoted as $X_{k1:n_k}, X_{k2:n_k}, \ldots, X_{kd_k:n_k}, k = 1, 2$, where

$$d_k = \begin{cases} r_{k1}, & \text{Case 1,} \\ m_{k2}, & \text{Cases 2 4,} \\ r_{k2}, & \text{Cases 3 5,} \\ m_{k1}, & \text{Case 6,} \end{cases}$$

where r_{k1} and r_{k2} represent the acquired number of failures before T_{k1} and T_{k2}, respectively.

Suppose that the lifetime of an item tested under normal operating conditions is assumed to follow the Weibull distribution, with the PDF, CDF, RF, and HRF given by Eqs. (1)–(3). In contrast,

under accelerated conditions, the HRF of a tested item is expressed as $H_2(x;\boldsymbol{\vartheta}) = \beta H_1(x;\mu,\theta)$, where $\boldsymbol{\vartheta} = (\mu,\beta,\theta)^\top$ is the unknown parameter vector, $H_1(x;\mu,\theta)$ is defined in Eq. (3) and β represents the acceleration factor satisfying $\beta > 1$. This means the failure rate is uniformly higher under accelerated stress. Consequently, the expected lifetime is shorter under stress. As a result, the HRF under accelerated conditions can be derived as follows

$$H_2(x;\boldsymbol{\vartheta}) = \mu\beta\theta x^{\theta-1}, x > 0, \mu,\theta > 0, \beta > 1. \tag{4}$$

The RF under accelerated conditions, denoted by $R_2(x;\boldsymbol{\vartheta})$, can be obtained using the HRF offered in (4) based on the relation $R_2(x;\boldsymbol{\vartheta}) = \exp\left\{-\int_0^x H_2(z;\boldsymbol{\vartheta})dz\right\}$, as

$$R_2(x;\boldsymbol{\vartheta}) = e^{-\mu\beta x^\theta}.$$

The related CDF and PDF can be expressed, respectively, as

$$F_2(x;\boldsymbol{\vartheta}) = 1 - e^{-\mu\beta x^\theta} \tag{5}$$

and

$$f_2(x;\boldsymbol{\vartheta}) = \mu\beta\theta x^{\theta-1} e^{-\mu\beta x^\theta}. \tag{6}$$

Let $x_{k1}, x_{k2}, \ldots, x_{kd_k}, k = 1, 2$ be the realization of the two UHC samples under CSPALTs $X_{k1:n_k}$, $X_{k2:n_k}, \ldots, X_{kd_k:n_k}$, with $x_{ki} = X_{ki:n_k}, i = 1, \ldots, d_k$ for simplicity. Then, the joint likelihood function of the observed data can be formulated as given below, without constant terms,

$$L(\boldsymbol{\vartheta};\underline{\mathbf{x}}) = \prod_{k=1}^{2}\left\{\prod_{i=1}^{d_k} f_k(x_{ki})\left[1 - F_k(\tau_k)\right]^{n_k-d_k}\right\}, \tag{7}$$

where $\underline{\mathbf{x}} = (x_{k1}, x_{k2}, \ldots, x_{kd_k})$. Fig. 1 outlines the complete framework of our study.

3 Classical Point and Interval Procedures

In the current section, the point and interval estimations of the model parameters, acceleration factor, and the two reliability metrics under normal operating conditions are discussed. Let $x_{11}, x_{12}, \ldots, x_{1d_1}$ be an observed UHC sample gathered from Weibull population at normal operating conditions with PDF and CDF given by (1) and (2), respectively. Additionally, let $x_{21}, x_{22}, \ldots, x_{2d_2}$ be an observed UHC sample collected from Weibull population at accelerated conditions with CDF and PDF as presented by (5) and (6), respectively. Then, the likelihood function of the unknown parameter vector $\boldsymbol{\vartheta}$ can be written using (7) as

$$L(\boldsymbol{\vartheta};\underline{\mathbf{x}}) = (\mu\theta)^D \beta^{d_2} \exp\left(-\mu\sum_{i=1}^{d_1} x_{1i}^\theta - \mu d_1^* \tau_1^\theta\right) \exp\left(-\mu\beta\sum_{i=1}^{d_2} x_{2i}^\theta - \mu\beta d_2^* \tau_2^\theta\right) \prod_{i=1}^{d_1} x_{1i}^{\theta-1} \prod_{i=1}^{d_2} x_{2i}^{\theta-1} \tag{8}$$

where $D = d_1 + d_2$ and $d_k^* = n_k - d_k$. After some simplifications, the likelihood function in (8) can be expressed as

$$L(\boldsymbol{\vartheta};\underline{\mathbf{x}}) = (\mu\theta)^D \beta^{d_2} \exp\left\{(\theta-1)\sum_{k=1}^{2}\sum_{i=1}^{d_k}\log(x_{ki}) - \mu\sum_{k=1}^{2}\sum_{i=1}^{d_k}\beta^{k-1}x_{ki}^\theta - \mu\sum_{k=1}^{2} d_k^*\beta^{k-1}\tau_k^\theta\right\} \tag{9}$$

The natural logarithm of (9) follows

$$l(\boldsymbol{\vartheta};\underline{\mathbf{x}}) = D\log(\mu\theta) + d_2\log(\beta) + (\theta-1)\sum_{k=1}^{2}\sum_{i=1}^{d_k}\log(x_{ki}) - \mu\sum_{k=1}^{2}\beta^{k-1}\left(\sum_{i=1}^{d_k}x_{ki}^{\theta} + d_k^{*}\tau_k^{\theta}\right) \tag{10}$$

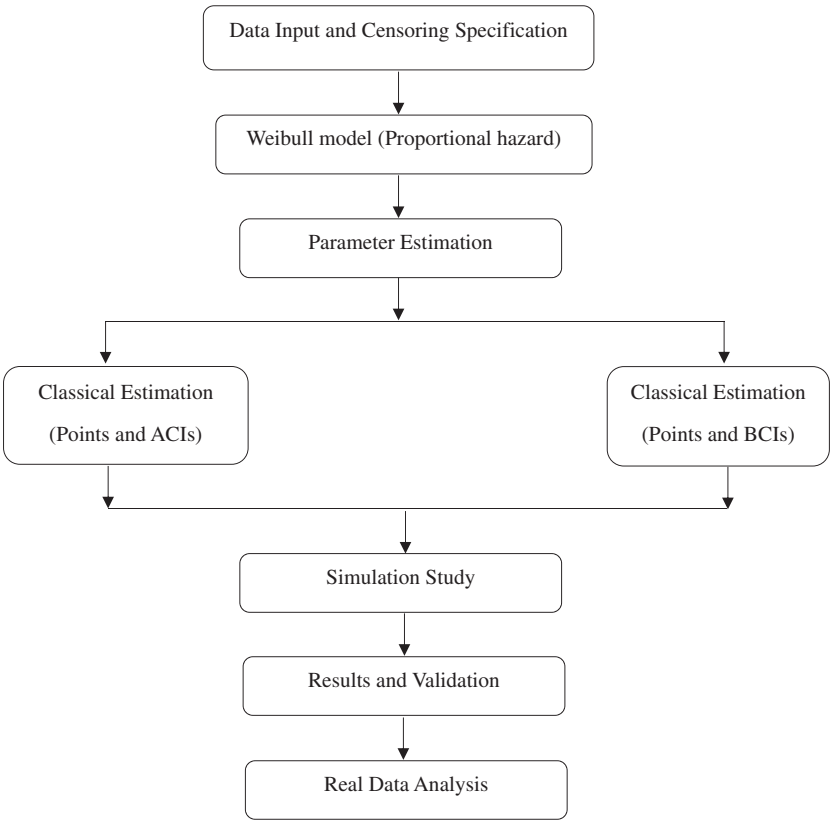

Figure 1: Weibull model analysis under UHC scheme with CSPALTs

By differentiating the log-likelihood function in (10) with respect to the parameters μ, β, and θ, the MLEs of these parameters can be obtained by solving the following three likelihood equations simultaneously

$$\frac{\partial l(\boldsymbol{\vartheta};\underline{\mathbf{x}})}{\partial\mu} = \frac{D}{\mu} - \sum_{k=1}^{2}\beta^{k-1}\left(\sum_{i=1}^{d_k}x_{ki}^{\theta} + d_k^{*}\tau_k^{\theta}\right) = 0, \tag{11}$$

$$\frac{\partial l(\boldsymbol{\vartheta};\underline{\mathbf{x}})}{\partial\beta} = \frac{d_2}{\beta} - \mu\left(\sum_{i=1}^{d_2}x_{2i}^{\theta} + d_2^{*}\tau_2^{\theta}\right) = 0 \tag{12}$$

and

$$\frac{\partial l(\boldsymbol{\vartheta};\underline{\mathbf{x}})}{\partial\theta} = \frac{D}{\theta} + \sum_{k=1}^{2}\sum_{i=1}^{d_k}\log(x_{ki}) - \mu\sum_{k=1}^{2}\beta^{k-1}\left(\sum_{i=1}^{d_k}x_{ki}^{\theta}\log(x_{ki}) + d_k^{*}\tau_k^{\theta}\log(\tau_k)\right) = 0. \tag{13}$$

It follows from (11) that the MLE of the scale parameter μ can be obtained as a function of the other two parameters as follows

$$\hat{\mu}(\beta,\theta)=\frac{D}{\sum_{k=1}^{2}\beta^{k-1}\left(\sum_{i=1}^{d_k}x_{ki}^{\theta}+d_k^{*}\tau_k^{\theta}\right)}. \tag{14}$$

By substituting $\hat{\mu}(\beta,\theta)$ in the normal equation in (12), after some simplifications one can easily obtain the MLE of the acceleration factor as a function of the shape parameter θ as follows

$$\hat{\beta}(\theta)=\frac{d_2\left(\sum_{i=1}^{d_1}x_{1i}^{\theta}+d_1^{*}\tau_1^{\theta}\right)}{d_1\left(\sum_{i=1}^{d_2}x_{2i}^{\theta}+d_2^{*}\tau_2^{\theta}\right)}. \tag{15}$$

The MLE of μ can be explicitly obtained as a function of the shape parameter only, after substituting $\hat{\beta}(\theta)$ into (14), as follows

$$\hat{\mu}(\theta)=\frac{d_1}{\sum_{i=1}^{d_1}x_{1i}^{\theta}+d_1^{*}\tau_1^{\theta}}. \tag{16}$$

By substituting $\hat{\beta}(\theta)$ and $\hat{\mu}(\theta)$ into Eq. (10), the profile log-likelihood of θ can be expressed as follows

$$l(\theta)=\sum_{k=1}^{2}d_k\log\left(\frac{\theta}{\sum_{i=1}^{d_k}x_{ki}^{\theta}+d_k^{*}\tau_k^{\theta}}\right)+\theta\sum_{k=1}^{2}\sum_{i=1}^{d_k}\log(x_{ki}). \tag{17}$$

The MLE of θ, denoted by $\hat{\theta}$, can be computed by maximizing Eq. (17) with respect to θ. By differentiating Eq. (17) with respect to θ and equating the result to zero yields the MLE $\hat{\theta}$. This results in the relationship $\theta=q(\theta)$, which takes the following form

$$q(\theta)=\left\{\sum_{k=1}^{2}\frac{d_k}{D}\left(\frac{\sum_{i=1}^{d_k}x_{ki}^{\theta}\log(x_{ki})+d_k^{*}\tau_k^{\theta}\log(\tau_k)}{\sum_{i=1}^{d_k}x_{ki}^{\theta}+d_k^{*}\tau_k^{\theta}}\right)-\frac{\sum_{k=1}^{2}\sum_{i=1}^{d_k}\log(x_{ki})}{D}\right\}^{-1}. \tag{18}$$

Using Eq. (18), the MLE of θ can be computed iteratively. Once $\hat{\theta}$ is obtained, the MLEs $\hat{\beta}$ and $\hat{\mu}$ can be straightforwardly calculated from (15) and (16), respectively. Based on to the invariance property of MLEs, the reliability characteristics under normal operating conditions at a specific time t can be derived from (3). This is achieved by substituting the original scale and shape parameters, μ and θ, with their respective MLEs, $\hat{\mu}$ and $\hat{\theta}$, as follows

$$\hat{R}_1(t)=e^{-\hat{\mu}t^{\hat{\theta}}}\quad\text{and}\quad\hat{H}_1(t)=\hat{\mu}\hat{\theta}t^{\hat{\theta}-1}.$$

In addition to acquiring point estimates for unknown parameters and reliability metrics under normal operating conditions, it is often essential to quantify the uncertainty associated with these estimates. This is achieved through interval estimation, which provides confidence regions likely to contain the true values with specified coverage probability. We employ the ACIs derived from the large-sample properties of the MLEs. Under some mild regularity conditions, the MLE vector $\hat{\boldsymbol{\vartheta}}=(\hat{\mu},\hat{\beta},\hat{\theta})^{\top}$ satisfies the asymptotic normality property, i.e., $\hat{\boldsymbol{\vartheta}}\sim N(\boldsymbol{\vartheta},\boldsymbol{I}^{-1}(\boldsymbol{\vartheta}))$, where $\boldsymbol{I}^{-1}(\boldsymbol{\vartheta})$ denotes the variance-covariance matrix. In practice, we approximate $\boldsymbol{I}^{-1}(\boldsymbol{\vartheta})$ through inverting the observed Fisher information matrix evaluated at the MLEs, as follows

$$\boldsymbol{I}^{-1}(\hat{\boldsymbol{\vartheta}}) = \begin{pmatrix} -l_{11} & -l_{12} & -l_{13} \\ & -l_{22} & -l_{23} \\ & & -l_{33} \end{pmatrix}^{-1}_{\boldsymbol{\vartheta}=\hat{\boldsymbol{\vartheta}}} = \begin{pmatrix} \hat{V}_{11} & \hat{V}_{12} & \hat{V}_{13} \\ & \hat{V}_{22} & \hat{V}_{23} \\ & & \hat{V}_{33} \end{pmatrix}, \tag{19}$$

where

$$l_{11} = -\frac{D}{\mu^2},\ l_{22} = -\frac{d_2}{\beta^2},\ l_{33} = -\frac{D}{\theta^2} - \mu \sum_{k=1}^{2} \beta^{k-1} \left(\sum_{i=1}^{d_k} x_{ki}^{\theta} \log^2(x_{ki}) + d_k^* \tau_k^{\theta} \log^2(\tau_k) \right),$$

$$l_{12} = -\sum_{i=1}^{d_2} x_{2i}^{\theta} + d_2^* \tau_2^{\theta},\ l_{13} = -\sum_{k=1}^{2} \beta^{k-1} \left(\sum_{i=1}^{d_k} x_{ki}^{\theta} \log(x_{ki}) + d_k^* \tau_k^{\theta} \log(\tau_k) \right)$$

and

$$l_{23} = -\mu \left(\sum_{i=1}^{d_2} x_{2i}^{\theta} \log(x_{2i}) + d_2^* \tau_2^{\theta} \log(\tau_2) \right).$$

The estimated variance-covariance matrix presented in (19) facilitates the construction of $(1-\gamma)100\%$ ACIs for the unknown parameters as

$$\hat{\mu} \pm z_{\gamma/2}\sqrt{\hat{V}_{11}},\ \hat{\beta} \pm z_{\gamma/2}\sqrt{\hat{V}_{22}} \quad \text{and} \quad \hat{\theta} \pm z_{\gamma/2}\sqrt{\hat{V}_{33}},$$

where $z_{\gamma/2}$ denotes the upper $\gamma/2$ quantile of the standard normal distribution.

To construct the ACIs for the RF and HRF under normal operating conditions, a key challenge is obtaining the associated variances of the MLEs for these two metrics. One effective method to approximate the required variances is the delta method. To implement this approach, we first need to calculate the first-order derivatives of the reliability metrics evaluated at the MLEs of the unknown parameters, as outlined below

$$\hat{R}_{\mu} = -t^{\hat{\theta}} e^{-\hat{\mu} t^{\hat{\theta}}}, \quad \hat{R}_{\theta} = -\hat{\mu} t^{\hat{\theta}} \log(t) e^{-\hat{\mu} t^{\hat{\theta}}},$$

and

$$\hat{h}_{\mu} = \hat{\theta} x^{\hat{\theta}-1},\ \hat{h}_{\theta} = \hat{\mu} t^{\hat{\theta}-1} [\hat{\theta} \log(t) + 1],$$

with $\hat{R}_{\beta} = \hat{h}_{\beta} = 0$. According to the delta method, the approximate variances can be computed as

$$\hat{V}_R = \begin{pmatrix} \hat{R}_{\mu} & 0 & \hat{R}_{\theta} \end{pmatrix} \boldsymbol{I}^{-1}(\hat{\boldsymbol{\vartheta}}) \begin{pmatrix} \hat{R}_{\mu} & 0 & \hat{R}_{\theta} \end{pmatrix}^{\top}$$
$$= \hat{R}_{\mu}^2 \hat{V}_{11} + 2\hat{R}_{\mu}\hat{R}_{\theta}\hat{V}_{13} + \hat{R}_{\theta}^2 \hat{V}_{33},$$

and

$$\hat{V}_h = \begin{pmatrix} \hat{h}_{\mu} & 0 & \hat{h}_{\theta} \end{pmatrix} \boldsymbol{I}^{-1}(\hat{\boldsymbol{\vartheta}}) \begin{pmatrix} \hat{h}_{\mu} & 0 & \hat{h}_{\theta} \end{pmatrix}^{\top}$$
$$= \hat{h}_{\mu}^2 \hat{V}_{11} + 2\hat{h}_{\mu}\hat{h}_{\theta}\hat{V}_{13} + \hat{h}_{\theta}^2 \hat{V}_{33}.$$

Hence, the $(1-\gamma)100\%$ ACIs for the two reliability metrics are

$$\hat{R}(t) \pm z_{\gamma/2}\sqrt{\hat{V}_R} \quad \text{and} \quad \hat{h}(t) \pm z_{\gamma/2}\sqrt{\hat{V}_h}.$$

4 Bayesian Estimation

The Bayes estimates and BCIs for the model parameters, the acceleration factor and the two reliability metrics, are examined in this section in the context of the UHC plan with CSPALTs. The point estimates are derived using the symmetric squared error loss function. It is assumed that the three random variables μ, β, and θ are independent, with gamma distributions serving as the prior distributions for the random variables μ and θ, while a non-informative prior is utilized for the random variable θ. Consequently, the joint prior distribution can be written as

$$g(\boldsymbol{\vartheta}) \propto \mu^{c_1-1}\theta^{c_2-1}\beta^{-1}\exp\{-v_1\mu - v_2\theta\}, \mu,\theta > 0, \beta > 1, \tag{20}$$

where the hyper-parameters $c_j,\ v_j > 0,\ j = 1,2$, are known. Combining the available data represented by the likelihood function in (9) with the prior knowledge provided by the joint prior distribution in (20), we can express the posterior distribution of the unknown parameter vector $\boldsymbol{\vartheta}$ as

$$W(\boldsymbol{\vartheta}|\underline{\mathbf{x}}) = \frac{1}{A}\mu^{D+c_1-1}\theta^{D+c_2-1}\beta^{d_2-1} \times \exp\left\{\theta\left[\sum_{k=1}^{2}\sum_{i=1}^{d_k}\log(x_{ki}) - v_2\right] - \mu\left[\sum_{k=1}^{2}\beta^{k-1}\left(\sum_{i=1}^{d_k}x_{ki}^{\theta} + d_k^{*}\tau_k^{\theta}\right) + v_1\right]\right\}, \tag{21}$$

where

$$A = \int_0^{\infty}\int_0^{\infty}\int_1^{\infty} L(\boldsymbol{\vartheta};\underline{\mathbf{x}})g(\boldsymbol{\vartheta})d\beta\, d\mu\, d\theta.$$

Under the squared error loss function defined as $\rho(\vartheta,\tilde{\vartheta}) = (\tilde{\vartheta}-\vartheta)^2$, where $\tilde{\vartheta}$ is the Bayes estimator of ϑ. The Bayes estimator under the squared error loss corresponds to the posterior mean. This choice of loss function offers several advantages: it often yields analytically tractable solutions across diverse estimation problems, facilitates direct connections with the widely used mean squared error criterion, and ensures symmetric treatment of over- and under-estimation errors. These properties collectively support the development of balanced and unbiased statistical inference. For simplicity, assume that $G(\boldsymbol{\vartheta})$ represents a function of the vector of unknown parameters $\boldsymbol{\vartheta}$. Clearly, $G(\boldsymbol{\vartheta})$ may correspond to one of the parameters or a combination of them, such as the RF or the HRF. The Bayes estimator of $G(\boldsymbol{\vartheta})$ can then be derived using the posterior distribution given in (21) as follows

$$\tilde{G}(\boldsymbol{\vartheta}) = \int_0^{\infty}\int_0^{\infty}\int_1^{\infty} G(\boldsymbol{\vartheta})\, W(\boldsymbol{\vartheta}|\underline{\mathbf{x}})d\beta\, d\mu\, d\theta. \tag{22}$$

Clearly, it is not possible to compute the Bayes estimator given (22) directly due to the complex nature of the posterior distribution. For this reason, the MCMC sampling approach is employed to obtain the Bayesian point estimates. Furthermore, the same methodology is utilized to construct the BCIs. The MCMC sampling procedure is a cornerstone computational tool in Bayesian inference, facilitating the numerical approximation of complex posterior distributions. Among the most used MCMC methodologies, two algorithms stand out for their importance in both theoretical advancements and practical applications, namely Gibbs sampling and the Metropolis-Hastings (MH)

algorithm. These computational techniques have become essential across various scientific disciplines, especially in statistical modeling and machine learning.

To apply the MCMC sampling procedure and to determine which algorithm will be utilized, it is essential to derive the full conditional distribution for each parameter. These distributions can be established using the posterior distribution as indicated in (21), as given below

$$W(\mu|\boldsymbol{\vartheta}_{-\mu},\underline{\mathbf{x}}) \propto \mu^{D+c_1-1}\exp\left\{-\mu\left[\sum_{k=1}^{2}\beta^{k-1}\left(\sum_{i=1}^{d_k}x_{ki}^{\theta}+d_k^{*}\tau_k^{\theta}\right)+v_1\right]\right\}, \tag{23}$$

$$W(\beta|\boldsymbol{\vartheta}_{-\beta},\underline{\mathbf{x}}) \propto \beta^{d_2-1}\exp\left\{-\mu\beta\left(\sum_{i=1}^{d_2}x_{2i}^{\theta}+d_2^{*}\tau_2^{\theta}\right)\right\}, \tag{24}$$

and

$$W(\theta|\boldsymbol{\vartheta}_{-\theta},\underline{\mathbf{x}}) \propto \theta^{D+c_2-1} \times \exp\left\{\theta\left[\sum_{k=1}^{2}\sum_{i=1}^{d_k}\log(x_{ki})-v_2\right]-\mu\sum_{k=1}^{2}\beta^{k-1}\left(\sum_{i=1}^{d_k}x_{ki}^{\theta}+d_k^{*}\tau_k^{\theta}\right)\right\}. \tag{25}$$

By examining the full conditional distributions in (23) and (24) to determine whether they belong to any well-known distributions, we can observe the following:

1. $\mu|\boldsymbol{\vartheta}_{-\mu},\underline{\mathbf{x}} \sim Gamma\left(D+c_1, \sum_{k=1}^{2}\beta^{k-1}\left(\sum_{i=1}^{d_k}x_{ki}^{\theta}+d_k^{*}\tau_k^{\theta}\right)+v_1\right)$.
2. $\beta|\boldsymbol{\vartheta}_{-\beta},\underline{\mathbf{x}} \sim Gamma\left(d_2, \mu\left(\sum_{i=1}^{d_2}x_{2i}^{\theta}+d_2^{*}\tau_2^{\theta}\right)\right)$.
3. The distribution $W(\theta|\boldsymbol{\vartheta}_{-\theta},\underline{\mathbf{x}})$ is unknown.

Consequently, obtaining MCMC samples from the conditional distributions of the scale parameter and the acceleration factor can be readily accomplished using any gamma generation routine. On the other hand, given that the conditional distribution of the shape parameter θ is unknown, we propose employing the MH algorithm. To implement this algorithm effectively, it is crucial to select an appropriate proposal distribution from which to sample. In this context, we have opted to utilize the normal distribution as the proposal distribution. This choice is substantiated by plotting the conditional distribution in (25) to support our selection. Therefore, we employ the MH within Gibbs algorithm to generate the MCMC samples related to μ, β, and θ. This is done to obtain the Bayes estimates (both point and interval) for any function related to these parameters. To implement the MH within Gibbs algorithm, we follow the steps outlined below for the sample generation process

Step 1: Start with intimal values of μ, β, and θ as $(\mu^{(0)},\beta^{(0)},\theta^{(0)})$. Here, we use the MLEs $\hat{\mu}$, $\hat{\beta}$, and $\hat{\theta}$, for this purpose.

Step 2: Set $a=1$.

Step 3: Simulate $\theta^{(a)}$ through implementing the following MH algorithm:

(1) Use $N(\theta^{(a-1)},\hat{V}_{33})$ to simulate a candidate value θ^{*}.

(2) Calculate $\zeta = \min\left\{1, \dfrac{W(\theta^{*}|\boldsymbol{\vartheta}_{-\theta}^{(a-1)},\underline{\mathbf{x}})}{W(\theta^{(a)}|\boldsymbol{\vartheta}_{-\theta}^{(a-1)},\underline{\mathbf{x}})}\right\}$.

(3) Obtain u from $U(0,1)$.

(4) Put $\theta^{(a)}=\theta^{*}$ if $u \leqslant \zeta$, otherwise put $\theta^{(a)}=\theta^{(a-1)}$.

Step 4: Generate $\mu^{(a)}$ using $Gamma\left(D+c_1, \sum_{k=1}^{2}[\beta^{k-1}]^{(a-1)}\left(\sum_{i=1}^{d_k} x_{ki}^{\theta^{(a)}} + d_k^* \tau_k^{\theta^{(a)}}\right) + v_1\right)$.

Step 5: Simulate $\beta^{(a)}$ using $Gamma\left(d_2, \mu^{(a)}\left(\sum_{i=1}^{d_2} x_{2i}^{\theta^{(a)}} + d_2^* \tau_2^{\theta^{(a)}}\right)\right)$.

Step 6: At iteration a, obtain the RF and HRF at normal operating conditions using the acquired $(\mu^{(a)}, \beta^{(a)}, \theta^{(a)})$ as

$$R_1^{(a)} = e^{-\mu^{(a)} t^{\theta^{(a)}}} \quad \text{and} \quad H_1^{(a)} = \mu^{(a)}\theta^{(a)} t^{\theta^{(a)}-1}.$$

Step 7: Replace a by $a+1$.

Step 8: Perform the steps 3 to 7, $\mathcal{M}$ times to collect:

$$\left\{\mu^{(a)}, \beta^{(a)}, \theta^{(a)}, R_1^{(a)}, H_1^{(a)}\right\}, a = 1, \ldots, \mathcal{M}.$$

The Bayes estimates and the BCIs can be obtained from the generated MCMC sequence. To ensure convergence and reduce the impact of initialization bias, the initial $\mathcal{Q}$ iterations are discarded as a burn-in phase. The Bayes estimates of the model parameters, the acceleration factor, and the two reliability metrics, in this context are given as

$$\tilde{\mu} = \frac{1}{\mathcal{M}-\mathcal{Q}}\sum_{a=\mathcal{Q}+1}^{\mathcal{M}} \mu^{(a)}, \quad \tilde{\beta} = \frac{1}{\mathcal{M}-\mathcal{Q}}\sum_{a=\mathcal{Q}+1}^{\mathcal{M}} \beta^{(a)}, \quad \tilde{\theta} = \frac{1}{\mathcal{M}-\mathcal{Q}}\sum_{a=\mathcal{Q}+1}^{\mathcal{M}} \theta^{(a)}$$

$$\tilde{R}_1(t) = \frac{1}{\mathcal{M}-\mathcal{Q}}\sum_{a=\mathcal{Q}+1}^{\mathcal{M}} R_1^{(a)}, \quad \text{and} \quad \tilde{H}_1(t) = \frac{1}{\mathcal{M}-\mathcal{Q}}\sum_{a=\mathcal{Q}+1}^{\mathcal{M}} H_1^{(a)}.$$

To Obtain the BCIs, we first sort the MCMC samples in ascending order as follows

$$\left\{\mu^{[\mathcal{Q}+1]} < \ldots < \mu^{[\mathcal{M}]}\right\}, \quad \left\{\beta^{[\mathcal{Q}+1]} < \ldots < \beta^{[\mathcal{M}]}\right\}, \quad \left\{\theta^{[\mathcal{Q}+1]} < \ldots < \theta^{[\mathcal{M}]}\right\},$$

$$\left\{R_1^{[\mathcal{Q}+1]} < \ldots < R_1^{[\mathcal{M}]}\right\}, \quad \text{and} \quad \left\{H_1^{[\mathcal{Q}+1]} < \ldots < H_1^{[\mathcal{M}]}\right\}.$$

Accordingly, the $100(1-\gamma)\%$ BCIs are constructed as follows:

$$\left\{\mu^{[\gamma(\mathcal{M}-\mathcal{Q})/2]}, \mu^{[(1-\gamma/2)(\mathcal{M}-\mathcal{Q})]}\right\}, \quad \left\{\beta^{[\gamma(\mathcal{M}-\mathcal{Q})/2]}, \beta^{[(1-\gamma/2)(\mathcal{M}-\mathcal{Q})]}\right\}, \quad \left\{\theta^{[\gamma(\mathcal{M}-\mathcal{Q})/2]}, \theta^{[(1-\gamma/2)(\mathcal{M}-\mathcal{Q})]}\right\}$$

$$\left\{R_1^{[\gamma(\mathcal{M}-\mathcal{Q})/2]}, R_1^{[(1-\gamma/2)(\mathcal{M}-\mathcal{Q})]}\right\}, \quad \text{and} \quad \left\{H_1^{[\gamma(\mathcal{M}-\mathcal{Q})/2]}, H_1^{[(1-\gamma/2)(\mathcal{M}-\mathcal{Q})]}\right\}.$$

5 Monte Carlo Comparisons

This section provides detailed Monte Carlo comparisons to examine how the point and interval estimators behave and to assess how well they estimate θ, μ, β, $R_1(t)$, and $H_1(t)$ mentioned earlier.

5.1 Simulation Setups

We now generate 1000 UHC with CSPALT samples when the actual values of (α, β, λ) (including Weibull parameters (θ, μ) and the acceleration operator β) are taken as Set-1:(1.5, 0.5, 1.5) and Set-2:(2.5, 1.5, 2.5). Making use of different options of n_i, $i = 1, 2$ (full sample size), m_{ij}, $i, j = 1, 2$ (effective sample size), and T_{ij}, $i, j = 1, 2$ (threshold time), all required UHC with CSPALT datasets are gathered. It is worth remembering here that $T_i \in (0, \infty)$ (for $i = 1, 2$) with $T_1 < T_2$, and $k, m \in \{1, 2, \ldots, n\}$ with $k < m$. In Table 1, by fixing $T_{11}(= 0.4, 0.8)$, $T_{12} = T_{21}(= 0.8, 1.5)$, and $T_{22}(= 1.5, 2.5)$, we specify several combinations of n_i, $i = 1, 2$, m_{ij}, $i, j = 1, 2$, and T_{ij}, $i,j = 1, 2$. At a specific time point, $t = 0.1$, the estimated values of $(R_1(t), H_1(t))$ under their normal operating systems are

evaluated, where their true values are considered as (0.9843, 0.2372) and (0.9953, 0.1186) from Set-1 and -2, respectively.

Table 1: Various Monte Carlo setups of Weibull model from UHC with CSPALT plan

Test	(n_1, n_2)	$\{(m_{11}, m_{12}), (m_{21}, m_{22})\}$
1	(20, 30)	{(5, 10), (10, 15)}
2		{(10, 15), (15, 25)}
3	(40, 50)	{(10, 20), (20, 30)}
4		{(20, 30), (30, 40)}
5	(60, 80)	{(20, 30), (30, 40)}
6		{(30, 40), (40, 60)}

After obtaining the required 1000 HUC samples, the MLEs and 95% ACIs for θ, μ, β, $R_1(t)$, and $H_1(t)$ are computed using the Newton-Raphson approach via the '`maxLik`' package introduced by Henningsen and Toomet [42]. For the Bayesian analysis, for Set-1 and -2, two prior groups of the hyperparameters (c_1, c_2, v_1, v_2) are utilized, namely:

- For Set-1:
  - Group-1: $(c_1, c_2) = (2.5, 7.5)$ and $v_i = 5,\ i = 1, 2$;
  - Group-2: $(c_1, c_2) = (5, 15)$ and $v_i = 10,\ i = 1, 2$.
- For Set-2:
  - Group-1: $(c_1, c_2) = (7.5, 12.5)$ and $v_i = 5,\ i = 1, 2$;
  - Group-2: $(c_1, c_2) = (15, 25)$ and $v_i = 10,\ i = 1, 2$.

All specified values of $(c_i, v_i),\ i = 1, 2$ for the prior knowledge of the Weibull populations used in Sets 1 and 2 are determined in such a way as to ensure that the prior means align with the corresponding actual values of θ and μ.

Next, beyond producing 12,000 MCMC samples of θ, μ, and β from (23)–(25), respectively, the first 2000 of them are discarded as burn-in. After that, using the '`coda`' package developed by Plummer et al. [43], the Bayes point estimates and 95% credible interval estimates using the MH-within-Gibbs sampler of θ, μ, β, $R_1(t)$, and $H_1(t)$ are computed.

In each simulation setup, the mean point estimates (MPEs) for β (as an example) are calculated by

$$\mathrm{MPE}(\breve{\beta}) = \frac{1}{1000}\sum_{i=1}^{1000}\breve{\beta}^{[i]},$$

where $\breve{\beta}^{[i]}$ is the estimate of β from the i-th simulated sample.

The point estimates are evaluated using the root mean squared errors (RMSEs) and mean relative absolute biases (MRABs), defined as

$$\mathrm{RMSE}(\breve{\beta}) = \sqrt{\frac{1}{1000}\sum_{i=1}^{1000}\left(\breve{\beta}^{[i]} - \beta\right)^2}$$

and

$$\mathrm{MRAB}(\check{\beta}) = \frac{1}{1000}\sum_{i=1}^{1000} \beta^{-1}\left|\check{\beta}^{[i]} - \beta\right|,$$

respectively.

The interval estimates are assessed through the average interval lengths (AILs) and coverage probabilities (CPs), computed as

$$\mathrm{AIL}^{95\%}(\beta) = \frac{1}{1000}\sum_{i=1}^{1000}\left(U_{\hat{\beta}[i]} - L_{\hat{\beta}[i]}\right),$$

and

$$\mathrm{CP}^{95\%}(\beta) = \frac{1}{1000}\sum_{i=1}^{1000} \mathrm{D}_{(L_{\hat{\beta}[i]}, U_{\hat{\beta}[i]})}(\beta),$$

where $\mathrm{D}(\cdot)$ denotes the indicator function, and $L(\cdot)$ and $U(\cdot)$ represent the lower and upper bounds of the 95% ACI or HPD intervals, respectively.

5.2 Simulation Results

Tables 2–6 present the MPEs, RMSEs, and MRABs in the first, second, and third columns, respectively, while Tables 7–11 report the AILs and CPs in their first and second columns, respectively.

From Tables 2–11, considering minimal RMSE, MRAB, and AIL values along with maximal CP values, the following behaviors are drawn:

- Generally, all calculated point and 95% interval estimates for θ, μ, β, $R_1(t)$, or $H_1(t)$ behaved well and reliably.
- Increasing $n_i,\ i = 1, 2$ improves inferential accuracy; a similar trend is observed when $m_{ij},\ i, j = 1, 2$ grow.
- The Bayes' estimates (or their 95% BCI estimates) for θ, μ, β, $R_1(t)$, or $H_1(t)$ outperform their classical MLE (or their 95% ACI estimates) counterparts due to the use of informative gamma priors.
- As the levels of θ, μ, and β increase, it is noted that:
  - The RMSEs, MRABs, and AILs for θ, μ, and $H_1(t)$ increase, while those of β and $R_1(t)$ decrease;
  - The CPs for θ, μ, and $H_1(t)$ decrease, while those of β and $R_1(t)$ increase.
- The calculated point/interval estimates of θ, μ, β, $R_1(t)$, and $H_1(t)$ developed from Set-1 behaved satisfactorily compared to those developed from Set-2.
- As thresholds $T_{ij},\ i, j = 1, 2$ increase, we noticed that the RMSEs, MRABs, and AILs for θ, μ, β, $R_1(t)$, and $H_1(t)$ narrowed down, while their CPs increase.
- All Bayes evaluations (created from point MCMC or BCI approach) against Group-2, which has a lower variance than Group-1, show better performance.
- To sum up, when a unified hybrid censored dataset is gathered from constant-stress partially accelerated life tests, the Bayesian approach via the MH-within-Gibbs algorithm is recommended for estimating model parameters and reliability characteristics in the Weibull lifetime model.

Table 2: The point estimation results of θ

$\{(m_{11}, m_{12}), (m_{21}, m_{22})\}$	Test	MLE			Bayes					
					Group-1			Group-2		
					Set-1					
{(0.4, 0.8), (0.8, 1.5)}	1	1.642	0.241	0.520	1.654	0.222	0.441	1.945	0.122	0.403
	2	1.602	0.222	0.461	1.586	0.205	0.399	1.904	0.112	0.245
	3	1.566	0.114	0.445	1.454	0.101	0.326	1.672	0.094	0.252
	4	1.560	0.108	0.372	1.444	0.092	0.299	1.600	0.090	0.235
	5	1.564	0.071	0.244	1.564	0.054	0.234	1.504	0.037	0.193
	6	1.536	0.073	0.249	1.588	0.071	0.229	1.532	0.053	0.184
{(0.8, 1.5), (1.5, 2.5)}	1	1.581	0.191	0.659	1.599	0.158	0.448	1.897	0.068	0.398
	2	1.578	0.173	0.630	1.540	0.147	0.445	1.791	0.067	0.369
	3	1.551	0.061	0.386	1.480	0.055	0.346	1.602	0.051	0.222
	4	1.543	0.060	0.383	1.435	0.053	0.345	1.582	0.045	0.216
	5	1.533	0.045	0.274	1.582	0.038	0.212	1.543	0.030	0.182
	6	1.526	0.041	0.267	1.554	0.032	0.207	1.505	0.027	0.172
					Set-2					
{(0.4, 0.8), (0.8, 1.2)}	1	2.624	0.259	0.527	2.671	0.236	0.468	2.951	0.130	0.436
	2	2.604	0.247	0.466	2.699	0.215	0.427	2.977	0.123	0.377
	3	2.575	0.134	0.534	2.407	0.109	0.397	2.748	0.097	0.311
	4	2.557	0.122	0.425	2.370	0.103	0.324	2.709	0.092	0.252
	5	2.545	0.080	0.269	2.620	0.077	0.236	2.553	0.057	0.193
	6	2.530	0.076	0.255	2.604	0.072	0.240	2.527	0.053	0.185
{(0.8, 1.5), (1.5, 2.5)}	1	2.606	0.220	0.683	2.612	0.160	0.493	2.892	0.076	0.426
	2	2.623	0.183	0.655	2.548	0.156	0.479	2.855	0.073	0.414
	3	2.561	0.069	0.449	2.411	0.061	0.384	2.737	0.053	0.240
	4	2.572	0.064	0.388	2.453	0.055	0.348	2.776	0.050	0.226
	5	2.530	0.048	0.300	2.605	0.037	0.249	2.534	0.033	0.198
	6	2.539	0.045	0.298	2.578	0.033	0.210	2.513	0.028	0.180

Table 3: The point estimation results of μ

$\{(m_{11}, m_{12}), (m_{21}, m_{22})\}$	Test	MLE			Bayes					
					Group-1			Group-2		
					Set-1					
{(0.4, 0.8), (0.8, 1.2)}	1	0.539	0.294	0.476	0.725	0.234	0.375	0.671	0.196	0.285
	2	0.543	0.251	0.357	0.651	0.212	0.325	0.591	0.163	0.248
	3	0.522	0.236	0.335	0.666	0.200	0.261	0.658	0.151	0.217
	4	0.523	0.224	0.278	0.636	0.187	0.238	0.603	0.133	0.200
	5	0.525	0.269	0.204	0.478	0.170	0.178	0.589	0.122	0.154
	6	0.517	0.333	0.199	0.486	0.151	0.159	0.597	0.105	0.140
{(0.8, 1.5), (1.5, 2.5)}	1	0.541	0.279	0.397	0.667	0.227	0.332	0.590	0.144	0.248
	2	0.509	0.243	0.326	0.641	0.194	0.281	0.543	0.138	0.234
	3	0.523	0.207	0.293	0.643	0.194	0.233	0.602	0.133	0.200
	4	0.503	0.211	0.246	0.615	0.185	0.203	0.573	0.110	0.172
	5	0.516	0.173	0.189	0.483	0.137	0.159	0.597	0.105	0.148
	6	0.503	0.168	0.163	0.466	0.136	0.142	0.573	0.091	0.137
					Set-2					
{(0.4, 0.8), (0.8, 1.2)}	1	1.766	0.927	0.369	1.907	0.550	0.323	1.780	0.511	0.275
	2	1.617	0.548	0.284	1.978	0.497	0.268	1.839	0.484	0.237
	3	1.627	0.509	0.262	1.758	0.438	0.228	1.977	0.347	0.180
	4	1.556	0.465	0.248	1.696	0.347	0.182	1.893	0.279	0.153
	5	1.586	0.363	0.182	1.543	0.314	0.155	1.773	0.182	0.076
	6	1.535	0.304	0.149	1.504	0.263	0.134	1.722	0.178	0.071
{(0.8, 1.5), (1.5, 2.5)}	1	1.608	0.553	0.324	1.904	0.550	0.318	1.766	0.476	0.254
	2	1.641	0.511	0.278	1.810	0.491	0.263	1.670	0.391	0.216
	3	1.557	0.468	0.233	1.730	0.356	0.205	1.926	0.302	0.172
	4	1.575	0.369	0.183	1.807	0.331	0.163	1.985	0.248	0.132
	5	1.531	0.352	0.179	1.507	0.278	0.145	1.731	0.184	0.071
	6	1.551	0.292	0.148	1.464	0.256	0.121	1.679	0.174	0.069

Table 4: The point estimation results of β

$\{(m_{11}, m_{12}), (m_{21}, m_{22})\}$	Test	MLE			Bayes					
					Group-1			Group-2		
					Set-1					
{(0.4, 0.8), (0.8, 1.2)}	1	1.784	1.127	0.439	1.097	0.784	0.283	1.191	0.576	0.256
	2	1.580	1.008	0.329	1.104	0.781	0.268	1.189	0.533	0.239
	3	1.597	0.763	0.289	1.360	0.490	0.251	1.751	0.454	0.226
	4	1.528	0.709	0.253	1.418	0.489	0.232	1.799	0.437	0.217
	5	1.560	0.579	0.220	1.802	0.379	0.147	1.300	0.182	0.118
	6	1.519	0.551	0.186	1.819	0.362	0.141	1.315	0.173	0.096
{(0.8, 1.5), (1.5, 2.5)}	1	1.576	0.976	0.329	1.108	0.703	0.269	1.180	0.463	0.221
	2	1.642	0.933	0.299	1.097	0.692	0.264	1.149	0.456	0.213
	3	1.520	0.691	0.261	1.451	0.465	0.230	1.805	0.447	0.203
	4	1.572	0.657	0.239	1.481	0.445	0.220	1.849	0.410	0.190
	5	1.516	0.534	0.183	1.822	0.357	0.134	1.333	0.177	0.084
	6	1.551	0.500	0.171	1.870	0.334	0.119	1.366	0.167	0.076
					Set-2					
{(0.4, 0.8), (0.8, 1.2)}	1	2.684	1.004	0.330	1.818	0.501	0.290	2.092	0.442	0.205
	2	2.742	0.662	0.303	1.831	0.454	0.277	2.100	0.399	0.192
	3	2.579	0.577	0.235	2.470	0.416	0.175	2.883	0.387	0.149
	4	2.625	0.446	0.219	2.465	0.410	0.174	2.891	0.363	0.137
	5	2.543	0.433	0.180	2.769	0.280	0.121	2.201	0.229	0.047
	6	2.585	0.356	0.172	2.803	0.270	0.115	2.217	0.202	0.046
{(0.8, 1.5), (1.5, 2.5)}	1	2.745	0.661	0.303	1.744	0.457	0.273	1.994	0.393	0.167
	2	2.681	0.613	0.298	1.744	0.447	0.268	2.029	0.356	0.164
	3	2.628	0.437	0.214	2.514	0.414	0.162	2.926	0.353	0.142
	4	2.589	0.418	0.202	2.493	0.406	0.156	2.926	0.335	0.128
	5	2.585	0.348	0.167	2.789	0.259	0.113	2.223	0.190	0.044
	6	2.549	0.332	0.156	2.816	0.236	0.106	2.242	0.189	0.044

Table 5: The point estimation results of $R_1(t)$

$\{(m_{11}, m_{12}), (m_{21}, m_{22})\}$	Test	MLE			Bayes					
					Group-1			Group-2		
					Set-1					
{(0.4, 0.8), (0.8, 1.2)}	1	0.985	0.231	0.111	0.981	0.207	0.088	0.989	0.118	0.082
	2	0.984	0.220	0.108	0.981	0.195	0.087	0.990	0.112	0.080
	3	0.984	0.106	0.088	0.976	0.090	0.070	0.986	0.080	0.048
	4	0.984	0.100	0.083	0.977	0.083	0.065	0.984	0.076	0.045
	5	0.985	0.068	0.054	0.987	0.055	0.045	0.981	0.046	0.036
	6	0.984	0.063	0.050	0.987	0.054	0.043	0.982	0.041	0.034
{(0.8, 1.5), (1.5, 2.5)}	1	0.984	0.216	0.107	0.981	0.195	0.088	0.990	0.103	0.079
	2	0.985	0.196	0.094	0.980	0.182	0.085	0.989	0.093	0.074
	3	0.984	0.096	0.073	0.978	0.085	0.062	0.985	0.077	0.045
	4	0.984	0.085	0.070	0.977	0.078	0.060	0.985	0.070	0.044
	5	0.984	0.060	0.048	0.987	0.054	0.044	0.982	0.043	0.036
	6	0.984	0.058	0.047	0.987	0.052	0.043	0.982	0.040	0.033
					Set-2					
{(0.4, 0.8), (0.8, 1.2)}	1	0.995	0.151	0.043	0.995	0.099	0.028	0.997	0.039	0.026
	2	0.995	0.119	0.039	0.995	0.101	0.028	0.997	0.037	0.023
	3	0.995	0.038	0.025	0.993	0.029	0.022	0.996	0.026	0.013
	4	0.995	0.034	0.028	0.993	0.027	0.021	0.996	0.025	0.014
	5	0.995	0.022	0.022	0.996	0.017	0.015	0.995	0.013	0.011
	6	0.995	0.022	0.017	0.996	0.016	0.012	0.995	0.012	0.010
{(0.8, 1.5), (1.5, 2.5)}	1	0.995	0.132	0.040	0.994	0.093	0.027	0.996	0.035	0.025
	2	0.995	0.117	0.036	0.994	0.092	0.025	0.996	0.033	0.021
	3	0.995	0.036	0.024	0.993	0.027	0.020	0.996	0.025	0.013
	4	0.995	0.031	0.022	0.993	0.026	0.019	0.996	0.021	0.012
	5	0.995	0.020	0.018	0.996	0.016	0.013	0.995	0.012	0.010
	6	0.995	0.020	0.015	0.996	0.015	0.012	0.995	0.011	0.009

Table 6: The point estimation results of $H_1(t)$

$\{(m_{11}, m_{12}), (m_{21}, m_{22})\}$	Test	MLE			Bayes					
					Group-1			Group-2		
					Set-1					
{(0.4, 0.8), (0.8, 1.2)}	1	0.221	0.220	0.527	0.289	0.160	0.468	0.175	0.076	0.436
	2	0.238	0.183	0.466	0.289	0.156	0.427	0.167	0.073	0.377
	3	0.231	0.069	0.445	0.343	0.061	0.384	0.238	0.053	0.311
	4	0.236	0.064	0.372	0.333	0.055	0.378	0.246	0.050	0.226
	5	0.231	0.045	0.244	0.203	0.035	0.219	0.282	0.031	0.183
	6	0.238	0.045	0.249	0.198	0.033	0.210	0.274	0.028	0.180
{(0.8, 1.5), (1.5, 2.5)}	1	0.240	0.191	0.520	0.290	0.158	0.441	0.168	0.068	0.398
	2	0.229	0.173	0.461	0.301	0.147	0.399	0.178	0.067	0.391
	3	0.238	0.061	0.534	0.318	0.055	0.326	0.245	0.051	0.222
	4	0.233	0.060	0.425	0.326	0.052	0.299	0.241	0.044	0.216
	5	0.238	0.042	0.269	0.199	0.038	0.212	0.269	0.029	0.182
	6	0.235	0.041	0.255	0.201	0.031	0.207	0.274	0.027	0.172
					Set-2					
{(0.4, 0.8), (0.8, 1.2)}	1	0.122	0.259	0.669	0.127	0.236	0.493	0.078	0.130	0.456
	2	0.120	0.247	0.630	0.126	0.215	0.479	0.077	0.123	0.414
	3	0.121	0.134	0.386	0.170	0.109	0.397	0.100	0.097	0.240
	4	0.121	0.122	0.383	0.175	0.103	0.324	0.103	0.092	0.252
	5	0.120	0.080	0.274	0.099	0.073	0.236	0.131	0.058	0.193
	6	0.120	0.076	0.267	0.099	0.072	0.240	0.133	0.053	0.185
{(0.8, 1.5), (1.5, 2.5)}	1	0.117	0.241	0.683	0.143	0.222	0.458	0.092	0.122	0.403
	2	0.117	0.222	0.655	0.149	0.205	0.445	0.088	0.112	0.245
	3	0.118	0.114	0.449	0.166	0.101	0.346	0.100	0.094	0.252
	4	0.117	0.108	0.488	0.160	0.092	0.345	0.095	0.090	0.251
	5	0.119	0.078	0.300	0.100	0.073	0.234	0.132	0.054	0.193
	6	0.119	0.073	0.298	0.102	0.071	0.229	0.133	0.048	0.184

Table 7: The 95% interval estimation of θ

$\{(m_{11}, m_{12}), (m_{21}, m_{22})\}$	Test	ACI		BCI			
				Group-1		Group-2	
				Set-1			
{(0.4, 0.8), (0.8, 1.2)}	1	1.298	0.922	0.970	0.926	0.645	0.932
	2	1.063	0.924	0.880	0.928	0.551	0.934
	3	0.880	0.928	0.550	0.932	0.522	0.938
	4	0.771	0.930	0.522	0.934	0.501	0.940
	5	0.735	0.931	0.446	0.935	0.424	0.941
	6	0.612	0.934	0.421	0.938	0.414	0.942
{(0.8, 1.5), (1.5, 2.5)}	1	0.982	0.925	0.860	0.930	0.541	0.934
	2	0.920	0.926	0.705	0.931	0.524	0.935
	3	0.716	0.930	0.543	0.935	0.517	0.939
	4	0.661	0.932	0.516	0.936	0.439	0.942
	5	0.564	0.935	0.441	0.940	0.418	0.944
	6	0.504	0.936	0.419	0.942	0.407	0.944
				Set-2			
{(0.4, 0.8), (0.8, 1.2)}	1	1.462	0.917	1.150	0.922	0.820	0.927
	2	1.238	0.921	1.127	0.926	0.799	0.931
	3	1.187	0.923	0.659	0.928	0.559	0.933
	4	1.048	0.925	0.655	0.929	0.543	0.934
	5	0.935	0.928	0.490	0.934	0.465	0.935
	6	0.830	0.930	0.468	0.936	0.440	0.938
{(0.8, 1.5), (1.5, 2.5)}	1	1.334	0.919	1.092	0.923	0.795	0.928
	2	1.129	0.923	1.082	0.927	0.779	0.932
	3	0.959	0.925	0.650	0.929	0.558	0.934
	4	0.918	0.926	0.627	0.931	0.533	0.934
	5	0.795	0.931	0.478	0.935	0.446	0.936
	6	0.688	0.933	0.460	0.937	0.437	0.938

Table 8: The 95% interval estimation of μ

$\{(m_{11}, m_{12}), (m_{21}, m_{22})\}$	Test	ACI		BCI			
				Group-1		Group-2	
				Set-1			
{(0.4, 0.8), (0.8, 1.2)}	1	1.137	0.934	0.808	0.936	0.689	0.941
	2	0.838	0.937	0.682	0.939	0.616	0.944
	3	0.641	0.939	0.588	0.941	0.504	0.945
	4	0.592	0.943	0.503	0.945	0.463	0.948
	5	0.504	0.946	0.459	0.947	0.430	0.950
	6	0.455	0.949	0.437	0.951	0.373	0.951
{(0.8, 1.5), (1.5, 2.5)}	1	0.819	0.935	0.746	0.939	0.681	0.942
	2	0.718	0.938	0.664	0.942	0.577	0.945
	3	0.591	0.940	0.542	0.944	0.463	0.947
	4	0.584	0.944	0.485	0.947	0.407	0.949
	5	0.460	0.947	0.444	0.950	0.372	0.951
	6	0.437	0.950	0.418	0.951	0.335	0.952
				Set-2			
{(0.4, 0.8), (0.8, 1.2)}	1	2.151	0.892	1.325	0.905	1.014	0.912
	2	1.972	0.895	1.304	0.908	0.994	0.915
	3	1.623	0.902	0.997	0.916	0.759	0.918
	4	1.358	0.907	0.920	0.921	0.635	0.924
	5	1.269	0.910	0.783	0.924	0.624	0.927
	6	1.096	0.916	0.730	0.929	0.611	0.928
{(0.8, 1.5), (1.5, 2.5)}	1	1.931	0.897	1.259	0.908	0.963	0.913
	2	1.873	0.900	1.207	0.911	0.947	0.916
	3	1.341	0.907	0.975	0.918	0.685	0.919
	4	1.168	0.912	0.894	0.923	0.626	0.925
	5	1.077	0.915	0.749	0.926	0.614	0.928
	6	1.004	0.920	0.646	0.931	0.605	0.928

Table 9: The 95% interval estimation of β

$\{(m_{11}, m_{12}), (m_{21}, m_{22})\}$	Test	ACI		BCI			
				Group-1		Group-2	
				Set-1			
{(0.4, 0.8), (0.8, 1.2)}	1	4.028	0.872	1.268	0.892	0.971	0.899
	2	3.882	0.876	1.217	0.898	0.906	0.903
	3	2.766	0.886	0.808	0.903	0.703	0.909
	4	2.697	0.889	0.760	0.908	0.698	0.911
	5	2.393	0.902	0.749	0.912	0.646	0.912
	6	2.142	0.905	0.730	0.912	0.602	0.914
{(0.8, 1.5), (1.5, 2.5)}	1	3.792	0.876	1.226	0.895	0.906	0.902
	2	3.369	0.880	1.182	0.901	0.868	0.908
	3	2.626	0.888	0.768	0.906	0.707	0.913
	4	2.405	0.901	0.730	0.910	0.685	0.914
	5	2.083	0.905	0.727	0.914	0.603	0.914
	6	1.955	0.907	0.685	0.913	0.572	0.915
				Set-2			
{(0.4, 0.8), (0.8, 1.2)}	1	2.767	0.884	1.253	0.894	0.936	0.900
	2	2.447	0.889	1.209	0.900	0.880	0.906
	3	2.196	0.892	0.718	0.905	0.694	0.911
	4	1.718	0.900	0.697	0.909	0.685	0.912
	5	1.671	0.902	0.622	0.913	0.402	0.917
	6	1.381	0.906	0.610	0.916	0.389	0.919
{(0.8, 1.5), (1.5, 2.5)}	1	2.397	0.888	1.221	0.896	0.876	0.903
	2	1.974	0.894	1.179	0.902	0.852	0.909
	3	1.664	0.899	0.697	0.907	0.680	0.914
	4	1.561	0.903	0.694	0.911	0.664	0.915
	5	1.336	0.907	0.619	0.915	0.400	0.920
	6	1.289	0.910	0.593	0.918	0.359	0.921

Table 10: The 95% interval estimation of $R_1(t)$

$\{(m_{11}, m_{12}), (m_{21}, m_{22})\}$	Test	ACI		BCI			
				Group-1		Group-2	
				Set-1			
{(0.4, 0.8), (0.8, 1.2)}	1	0.595	0.932	0.538	0.935	0.435	0.938
	2	0.569	0.933	0.515	0.936	0.412	0.939
	3	0.350	0.941	0.271	0.944	0.236	0.947
	4	0.303	0.942	0.265	0.945	0.219	0.948
	5	0.258	0.944	0.212	0.947	0.125	0.950
	6	0.248	0.945	0.209	0.948	0.120	0.951
{(0.8, 1.5), (1.5, 2.5)}	1	0.563	0.933	0.504	0.936	0.390	0.939
	2	0.519	0.934	0.469	0.937	0.359	0.940
	3	0.290	0.942	0.264	0.945	0.223	0.949
	4	0.277	0.943	0.239	0.946	0.207	0.950
	5	0.233	0.945	0.208	0.948	0.123	0.952
	6	0.229	0.946	0.194	0.949	0.119	0.952
				Set-2			
{(0.4, 0.8), (0.8, 1.2)}	1	0.346	0.941	0.241	0.946	0.154	0.952
	2	0.237	0.947	0.216	0.951	0.140	0.954
	3	0.158	0.952	0.118	0.955	0.107	0.958
	4	0.105	0.954	0.079	0.957	0.065	0.961
	5	0.095	0.955	0.064	0.958	0.044	0.962
	6	0.084	0.957	0.043	0.960	0.040	0.962
{(0.8, 1.5), (1.5, 2.5)}	1	0.302	0.943	0.220	0.947	0.133	0.953
	2	0.229	0.948	0.205	0.951	0.126	0.956
	3	0.126	0.953	0.080	0.956	0.086	0.961
	4	0.094	0.955	0.071	0.957	0.060	0.962
	5	0.082	0.956	0.048	0.959	0.038	0.963
	6	0.077	0.958	0.042	0.960	0.035	0.964

Table 11: The 95% interval estimation of $H_1(t)$

$\{(m_{11}, m_{12}), (m_{21}, m_{22})\}$	Test	ACI		BCI			
				Group-1		Group-2	
				Set-1			
{(0.4, 0.8), (0.8, 1.2)}	1	0.515	0.948	0.406	0.951	0.286	0.955
	2	0.396	0.953	0.376	0.955	0.268	0.959
	3	0.274	0.955	0.170	0.957	0.133	0.961
	4	0.214	0.957	0.160	0.959	0.130	0.963
	5	0.197	0.959	0.110	0.962	0.088	0.966
	6	0.173	0.960	0.097	0.963	0.075	0.967
{(0.8, 1.5), (1.5, 2.5)}	1	0.466	0.950	0.379	0.953	0.268	0.956
	2	0.339	0.954	0.357	0.957	0.259	0.960
	3	0.220	0.956	0.162	0.959	0.128	0.962
	4	0.186	0.958	0.145	0.961	0.112	0.965
	5	0.160	0.961	0.101	0.963	0.075	0.967
	6	0.152	0.962	0.095	0.965	0.071	0.967
				Set-2			
{(0.4, 0.8), (0.8, 1.2)}	1	0.700	0.942	0.633	0.945	0.493	0.952
	2	0.667	0.943	0.601	0.946	0.488	0.953
	3	0.397	0.950	0.332	0.953	0.312	0.960
	4	0.360	0.952	0.330	0.955	0.276	0.961
	5	0.308	0.955	0.281	0.957	0.186	0.963
	6	0.296	0.956	0.269	0.958	0.156	0.965
{(0.8, 1.5), (1.5, 2.5)}	1	0.662	0.944	0.589	0.947	0.469	0.954
	2	0.604	0.945	0.544	0.948	0.436	0.955
	3	0.367	0.952	0.331	0.955	0.266	0.962
	4	0.333	0.954	0.301	0.956	0.246	0.964
	5	0.284	0.956	0.272	0.959	0.158	0.965
	6	0.276	0.957	0.266	0.960	0.135	0.966

6 Real-World Applications

This section analyzes two separate applications using different accelerated datasets collected from the engineering and clinical fields to investigate how the estimating approaches suggested in the preceding sections operate in reality: one representing the failure times of white organic light-emitting diodes and the other representing the lifetime of micro-droplets in the ambient environment.

6.1 Light-Emitting Diode

Light-emitting diodes (LEDs) are extensively utilized among various types of semiconductor diodes and are commonly found in televisions and color displays. An LED is created from a very thin layer of heavily doped semiconductor material. Depending on the specific semiconductor material and the level of doping used, the forward-bias LED emits colored light at a distinct spectral wavelength. Using two CSALTs, namely 9.64 mA (normal-use condition) and 17.09 mA (stress condition), this application examines the lifetime of ten M00071 white organic LEDs (WOLEDs) mixed with three different colors, namely red, green, and blue. This dataset was originally provided by Zhang et al. [44] and reanalyzed later by Nassar et al. [45] and Nassar et al. [46]. For computational ease, for both datasets created by the given two stresses, 9.64 and 17.09 mA, each failure time point is divided by one thousand; see Table 12.

Table 12: Failures of 10 WOLEDs

Normal-use data									
1.6915	2.0847	2.1003	2.3745	2.4215	2.5860	2.6215	2.6805	2.8680	2.8795
Accelerated stress data									
0.6015	0.6897	0.6973	0.7165	0.7855	0.8545	0.8895	1.1157	1.1313	1.2515

To determine if the Weibull distribution is an adequate model to match the WOLED data, the Kolmogorov–Smirnov (K–S) distance and its related p-value (at 5% significance level) are acquired. To do this, the MLEs (with their standard error (Std.Es)) and associated 95% ACIs (with their interval widths (IWs)) of Weibull distribution parameters θ and μ, and Kolmogorov–Smirnov (KS) distance (with its p-value) are computed; see Table 13. It demonstrates that the Weibull lifespan distribution matches the WOLED data satisfactorily. Using several goodness-of-fit visualization tools, using both normal-use and accelerated conditions data sets, the estimated/empirical RF, probability-probability (PP), quantile-quantile (QQ), and scaled-TTT plots are shown in Fig. 2. It is evident, from the subplots in Fig. 2a–c, that given Weibull distribution gives an adequate fit to both normal-use and accelerated stress datasets as well. Fig. 2d reveals that the given WOLED datasets provide an increasing failure rate, which is one of the theoretical Weibull failure rates. Furthermore, to confirm the existence and uniqueness of the fitted values $\hat{\theta}$ and $\hat{\mu}$ (reported in Table 13), the log-likelihood contours for several choices of θ and μ using both WOLED datasets are depicted in Fig. 3. For next computations based on the WOLED dataset, we recommend using $\hat{\theta}$ and $\hat{\mu}$ calculated by normal-use and accelerated stress datasets as initial guesses.

Table 13: Fitting the Weibull (θ, μ) model from WOLED data

Stress	Par.	MLE (Std.E)	95% ACI[IW]	K–S (p-value)
9.64 mA	θ	6.4327 (0.5344)	(5.3854, 7.4801) [2.0947]	0.1878 (0.8102)
	μ	0.0026 (0.0011)	(0.0004, 0.0048) [0.0044]	
17.09 mA	θ	4.4606 (1.0765)	(2.3507, 6.5704) [2.0947]	0.1866 (0.8163)
	μ	1.2145 (0.3922)	(0.4457, 1.9833) [1.5376]	

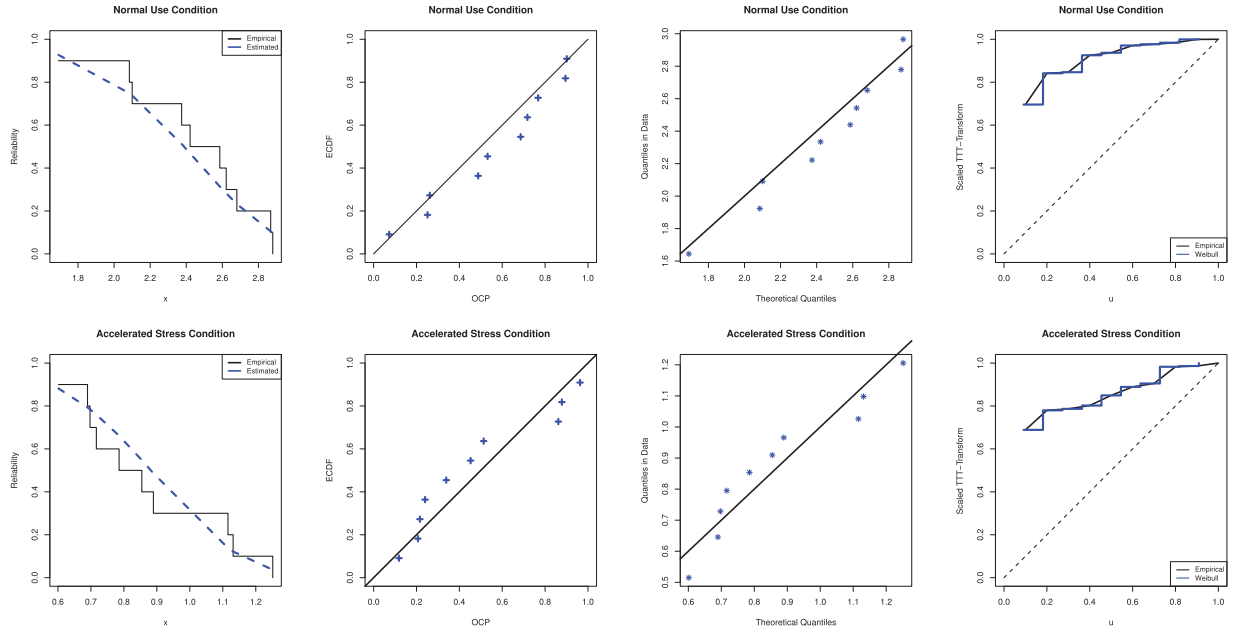

(a) RF (b) PP (c) QQ (d) TTT

Figure 2: Fitting diagrams of the Weibull model using WOLED data: (**a**) RF, (**b**) PP, (**c**) QQ, and (**d**) TTT plots

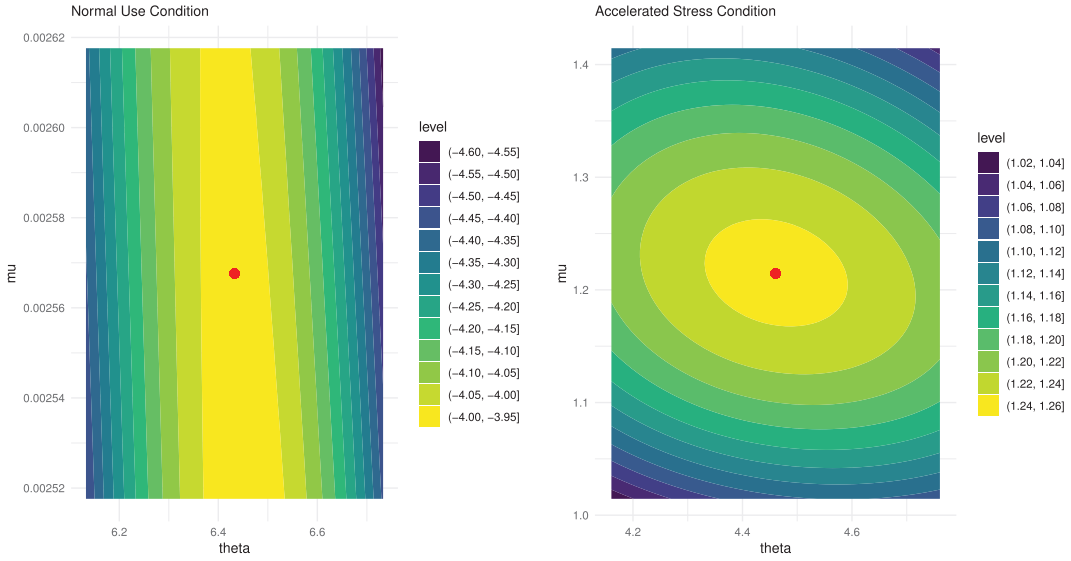

Figure 3: Contours of the Weibull parameters using WOLED data for normal use conditions (left panel), and accelerated conditions (right panel)

Now, by taking $(m_{11}, m_{12}) = (3, 6)$ and $(m_{21}, m_{22}) = (4, 8)$, three UHC samples with CSPALT using different thresholds T_{ij}, $i,j = 1,2$, are generated; see Table 14. For $\mathbb{S}i$, $i = 1,2,3$, the MLEs and associated 95% ACIs of θ, μ, β, $R_1(t)$, and $H_1(t)$ (at $t = 1.5$) are obtained. Since there is no available prior information on the Weibull parameters θ and μ from the given WOLED datasets, the hyperparameters of c_i and v_i (for $i = 1,2$) are utilized as improper, and each of them is set to be 0.001. This setting implies that the prior gamma densities are almost non-informative. Setting $\mathcal{M} = 50{,}000$ and $\mathcal{Q} = 10{,}000$ as burn-in in the MCMC procedures presented in Section 4, the Bayes' MCMC point estimates and related 95% BCI estimates of θ, μ, β, $R_1(t)$, and $H_1(t)$ are computed. The initial guesses of θ, μ, and β for running the MCMC sampler are assumed to be their frequentist estimates. In Table 15, the classical and Bayes point estimates (in addition to their Std.Es) as well as the asymptotic and credible interval estimates (in addition to their IWs) are reported. In terms of smallest Std.Es and shortest IWs, Table 15 shows that the Bayesian point (or credible) estimates perform well compared to those obtained from the frequentist approach. Furthermore, the findings summarized in Table 15 reinforce the same conclusions discussed in Section 5.

Table 14: Artificial UHC samples using CSPALT from WOLED data

Sample	(τ_1, τ_2)	$(T_{11}(r_{11}),\ T_{12}(r_{12}))$ $(T_{21}(r_{21}),\ T_{22}(r_{22}))$	Data
$\mathcal{S}1$	(2.7, 1.1157)	(2.7(8), 2.8(8))	$x_{1i} = 1.6915, 2.0847, 2.1003, 2.3745, 2.4215, 2.5860, 2.6215, 2.6805$
		(0.8(5), 1.2(8))	$x_{2i} = 0.6015, 0.6897, 0.6973, 0.7165, 0.7855, 0.8545, 0.8895, 1.1157$
$\mathcal{S}2$	(2.5860, 0.9)	(2.1(2), 2.6(6))	$x_{1i} = 1.6915, 2.0847, 2.1003, 2.3745, 2.4215, 2.5860$
		(0.7(3), 0.9(6))	$x_{2i} = 0.6015, 0.6897, 0.6973, 0.7165, 0.7855, 0.8545$

(Continued)

Table 14 (continued)

Sample	(τ_1, τ_2)	$(T_{11}(r_{11}),\ T_{12}(r_{12}))$ $(T_{21}(r_{21}),\ T_{22}(r_{22}))$	Data
$\mathcal{S}3$	(2.1003, 0.8)	(2.0(1), 2.1(2)) (0.7(3), 0.8(4))	$x_{1i} = 1.6915, 2.0847, 2.1003$ $x_{2i} = 0.6015, 0.6897, 0.6973, 0.7165, 0.7855$

Table 15: Estimates of θ, μ, β, $R_1(t)$, and $H_1(t)$ from WOLED data

Sample	Par.	MLE MCMC		95% ACI 95%		
		Est.	Std.E	Low.	Upp.	IW
$\mathcal{S}1$	θ	2.0725	0.9240	0.2616	3.8834	3.6218
		2.0726	0.0199	2.0334	2.1123	0.0789
	μ	0.0501	0.0021	0.0460	0.0543	0.0083
		0.0517	0.0108	0.0325	0.0739	0.0414
	β	20.824	56.251	0.0000	55.380	55.380
		20.824	0.0200	20.785	20.864	0.0790
	$R_1(t)$	0.8903	0.0349	0.8220	0.9587	0.1367
		0.8875	0.0220	0.8428	0.9274	0.0846
	$H_1(t)$	0.1605	0.1256	0.0000	0.4067	0.4067
		0.1654	0.0345	0.1041	0.2362	0.1321
$\mathcal{S}2$	θ	2.0743	1.0843	0.0000	4.1995	4.1995
		2.0735	0.0501	1.9753	2.1721	0.1968
	μ	0.0994	0.0061	0.0875	0.1113	0.0238
		0.1040	0.0255	0.0598	0.1574	0.0976
	β	3.0254	5.5184	0.0000	13.841	13.841
		3.0256	0.0500	2.9274	3.1225	0.1952
	$R_1(t)$	0.7942	0.0725	0.6522	0.9362	0.2841
		0.7871	0.0456	0.6954	0.8701	0.1747
	$H_1(t)$	0.3186	0.2924	0.0000	0.8916	1.1460
		0.3332	0.0815	0.1928	0.5022	0.3094
$\mathcal{S}3$	θ	1.6999	0.9145	0.0000	3.4923	3.4923
		1.6998	0.0499	1.6025	1.7979	0.1954
	μ	0.0878	0.0053	0.0773	0.0983	0.0210
		0.0931	0.0268	0.0471	0.1494	0.1023
	β	3.0026	6.5897	0.0000	15.918	15.918
		3.0026	0.0499	2.9045	3.1010	0.1965
	$R_1(t)$	0.8396	0.0500	0.7416	0.9375	0.1959
		0.8318	0.0437	0.7428	0.9101	0.1674

(Continued)

Table 15 (continued)

Sample	Par.	MLE MCMC		95% ACI 95%		
		Est.	Std.E	Low.	Upp.	IW
	$H_1(t)$	0.1982	0.1736	0.0000	0.5385	0.5385
		0.2102	0.0607	0.1064	0.3388	0.2325

Now, from $\mathcal{S}1$ in Table 14 as a representative case, we added a derivation showing how the UHC likelihood-based is as follows:

$$L(\boldsymbol{\vartheta};\underline{\mathbf{x}}) = (\mu\theta)^{16}\beta^{8}\exp\left(-\mu\sum_{i=1}^{9}x_{1i}^{\theta}-2\mu\tau_1^{\theta}\right)\exp\left(-\mu\beta\sum_{i=1}^{9}x_{2i}^{\theta}-2\mu\beta\tau_2^{\theta}\right)\prod_{i=1}^{8}x_{1i}^{\theta-1}\prod_{i=1}^{8}x_{2i}^{\theta-1},$$

where x_{ki} (for $k=1,2$) are available in Table 14.

To assess the existence and uniqueness of the likelihood estimates of θ, μ, and β from Samples $\mathcal{S}i$, $i=1,2,3$, the corresponding contour plots are presented in Fig. 4. These plots confirm that the fitted likelihood estimates of θ, μ, and β based on all samples reported in Table 14 exist and are unique. They also validate the numerical results reported in Table 15. Therefore, we recommend using these estimates as initial values for subsequent MCMC computational procedures. Fig. 5 displays the Gaussian kernel density estimates and trace plots (using Sample $\mathcal{S}1$ as an example) for the 40,000 MCMC samples of θ, μ, β, $R_1(t)$, and $H_1(t)$. The plots show good mixing behavior of the MCMC chains. The posterior iterations of θ and β appear reasonably symmetric, those of μ and $H_1(t)$ are positively skewed, while those of $R_1(t)$ are negatively skewed. These results suggest that the chosen burn-in period is sufficient to mitigate initial value effects and ensure proper mixing of the simulated samples. Various properties, namely mean, mode, and three quartiles Q_i, $i=1,2,3$, standard deviation (SD) and skewness (Sk.) from 40,000 MCMC variates of θ, μ, β, $R_1(t)$, and $H_1(t)$ are computed; see Table 16. It supports the same findings listed in Table 15 and the same facts shown in Fig. 5.

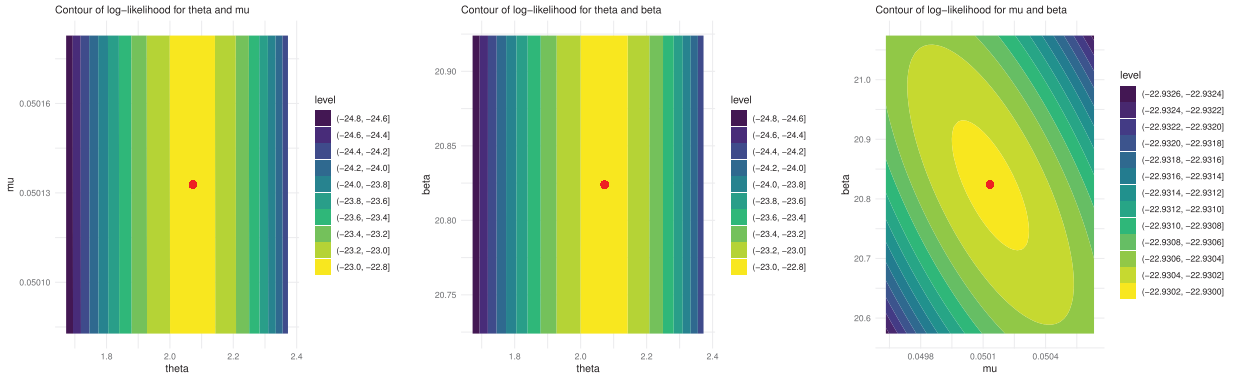

(a) Sample $\mathcal{S}1$

Figure 4: (Continued)

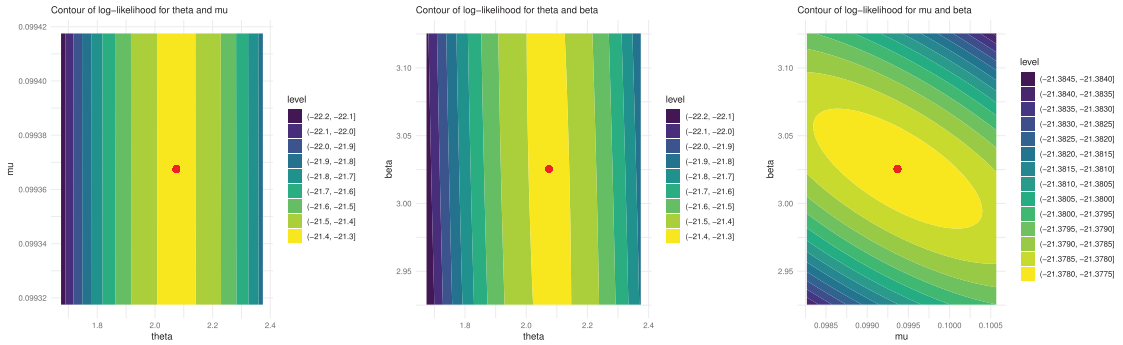

(b) Sample $\mathcal{S}2$

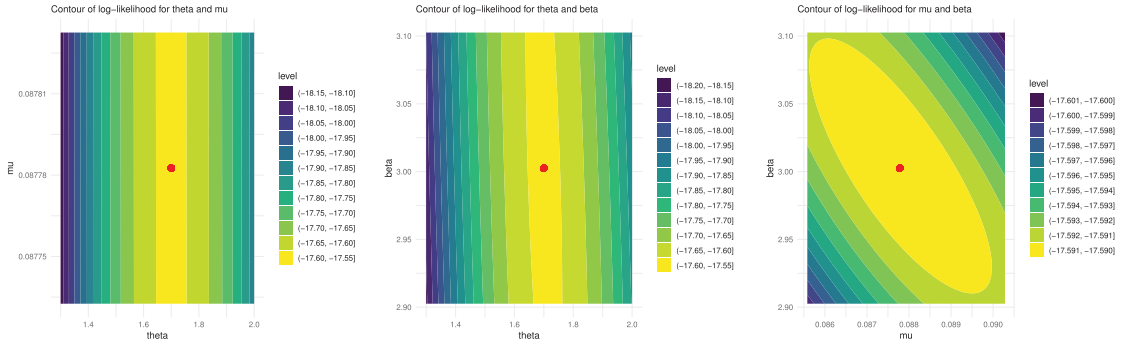

(c) Sample $\mathcal{S}3$

Figure 4: Likelihood contours of θ (left), μ (middle), and β (right) from WOLED data: (**a**) Sample $\mathcal{S}1$, (**b**) Sample $\mathcal{S}2$, and (**c**) Sample $\mathcal{S}3$

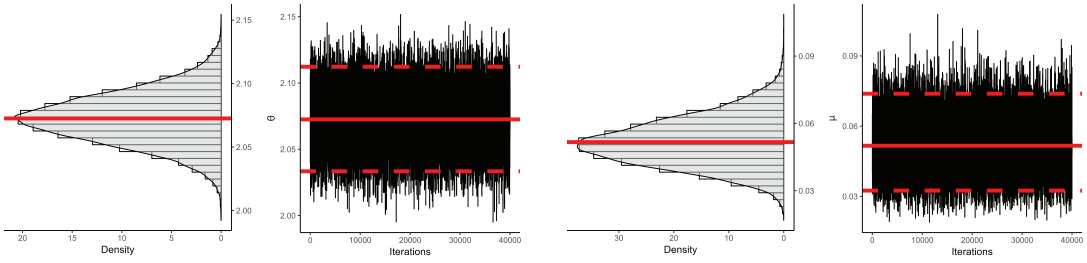

(a) θ (b) μ

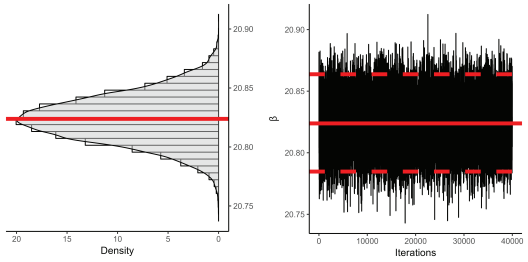

(c) β

Figure 5: (Continued)

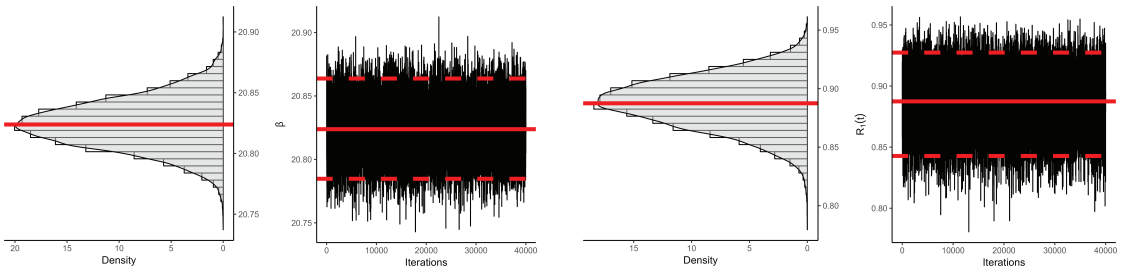

(d) $R_1(t)$ (e) $H_1(t)$

Figure 5: Density (left) and Trace (right) of θ, μ, β, $R_1(t)$, and $H_1(t)$ from WOLED data: **(a)** θ, **(b)** μ, **(c)** β, **(d)** $R_1(t)$, and **(e)** $H_1(t)$

Table 16: Statistics of θ, μ, β, $R_1(t)$, and $H_1(t)$ from WOLED data

Sample	Par.	Mean	Q_1	Q_2	Q_3	Mode	SD	Sk.
$\mathcal{S}1$	θ	2.0726	2.0726	2.0592	2.0726	2.0859	0.0199	0.0257
	μ	0.0517	0.0609	0.0441	0.0511	0.0587	0.0107	0.2964
	β	20.824	20.811	20.810	20.824	20.837	0.0200	0.0390
	$R_1(t)$	0.8875	0.8684	0.8730	0.8883	0.9029	0.0218	−0.2251
	$H_1(t)$	0.1654	0.1950	0.1411	0.1635	0.1876	0.0341	0.3007
$\mathcal{S}2$	θ	2.0735	1.9727	2.0396	2.0736	2.1070	0.0501	0.0197
	μ	0.1040	0.1017	0.0861	0.1024	0.1202	0.0250	0.3696
	β	3.0256	2.9566	2.9915	3.0249	3.0602	0.0500	−0.0051
	$R_1(t)$	0.7871	0.7975	0.7567	0.7889	0.8188	0.0450	−0.1957
	$H_1(t)$	0.3332	0.2975	0.2763	0.3274	0.3852	0.0801	0.3745
$\mathcal{S}3$	θ	1.6998	1.7409	1.6658	1.6994	1.7332	0.0499	0.0317
	μ	0.0931	0.0886	0.0746	0.0912	0.1099	0.0263	0.4041
	β	3.0026	2.9604	2.9693	3.0019	3.0363	0.0499	0.0115
	$R_1(t)$	0.8318	0.8356	0.8035	0.8337	0.8619	0.0430	−0.2462
	$H_1(t)$	0.2102	0.2084	0.1684	0.2060	0.2477	0.0595	0.4103

6.2 Micro-Droplets

Micro-droplets are a significant vector for transmitting infectious agents, including serious respiratory diseases. When a person sneezes, they release fine particles, typically around 10 μm in size, into the air. These particles can remain suspended, carrying viruses and other pathogens. When inhaled, they facilitate the spread of infection. As a preventive measure, individuals should avoid touching unfamiliar objects, proximity to others, and spending time in contaminated spaces. Airflow velocity directly affects how long these micro-droplets persist in the air; increasing or decreasing the airflow can shorten or extend their airborne lifetime; see Aliabadi et al. [47].

In this application, we examine the behavior of droplet diameters (in meters per second) under different airflow conditions. Following Asadi et al. [48], we treat measurements at an air velocity of 0.35 m/s (with sample size $n_1 = 15$) as data under normal-use, and measurements at 0.2 m/s (with sample size $n_2 = 19$) as data under accelerated conditions; see Table 17. Recently, this dataset has been reanalyzed under the inverse Weibull model by Nassar and Elshahhat [49].

Table 17: Times of micro-droplets in air

Normal use condition (0.35 m/s)									
Accelerated stress condition (0.20 m/s)									
0.94	1.08	1.10	1.60	1.92	2.28	2.48	2.60	2.76	3.00
3.22	3.22	3.40	3.58	3.60					
1.60	1.80	1.94	2.02	2.18	2.30	2.30	2.30	2.36	2.44
2.50	2.54	2.58	2.60	2.62	2.68	2.72	2.74	2.80	

To assess whether the Weibull distribution appropriately models the micro-droplets data, we apply the K–S test and calculate the corresponding p-value (at a 5% significance level). Using Table 17, we first compute the MLEs of the Weibull parameters θ and μ, along with their Std.Es; see Table 18. The results reported in Table 18 confirm that the Weibull distribution provides a good fit for the micro-droplet datasets. Again, using both normal-use and accelerated conditions datasets, Fig. 6a–c supports the fitting outcomes reported in Table 18 and shows that the considered Weibull distribution produces a suitable fit to the micro-droplets datasets superiorly. Fig. 6d states that the used datasets provide increasing failure rates, as also shown in Fig. 2d. Fig. 7 confirms the existence and uniqueness of the fitted values of $\hat{\theta}$ and $\hat{\mu}$ and supports the same fitting results reported in Table 18.

Table 18: Fitting the Weibull (θ, μ) model from micro-droplets data

Stress	Par.	MLE (Std.E)	95% ACI[IW]	K–S (p-value)
0.35 m/s	θ	3.1634 (0.6955)	(1.8002, 4.5267) [2.7264]	0.1463 (0.9051)
	μ	0.3656 (0.1451)	(0.0813, 0.6500) [0.5687]	
0.20 m/s	θ	9.5117 (1.8186)	(5.9508, 13.073) [2.0947]	0.1034 (0.9872)
	μ	0.1178 (0.0626)	(0.0013, 0.2406) [0.2393]	

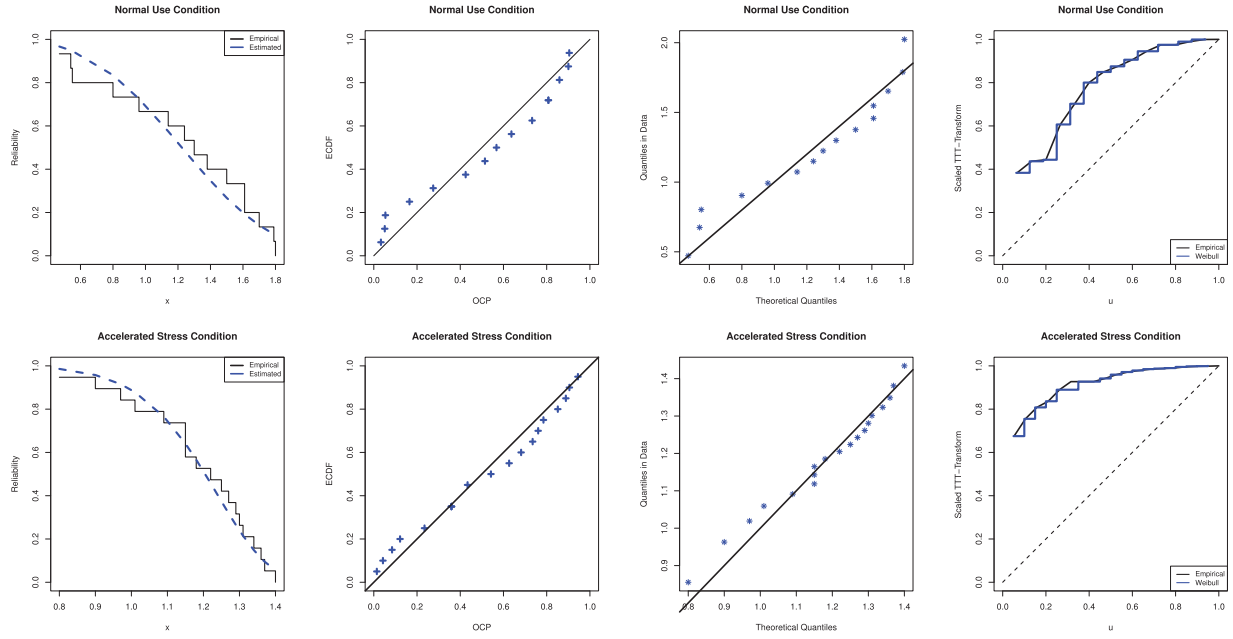

(a) RF (b) PP (c) QQ (d) TTT

Figure 6: Fitting diagrams of the Weibull model using micro-droplets data: (**a**) RF, (**b**) PP, (**c**) QQ, and (**d**) TTT plots

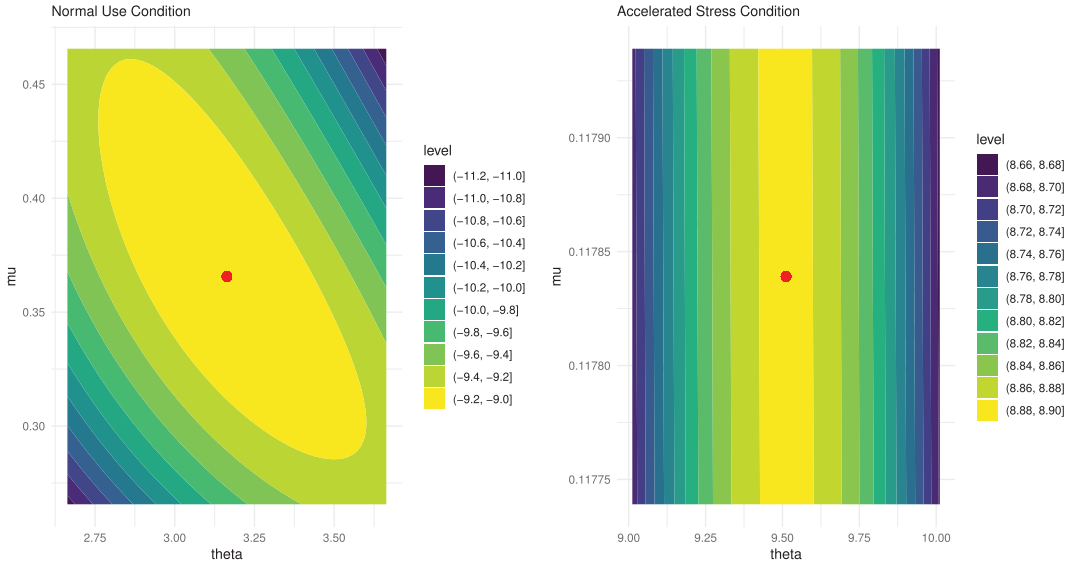

Figure 7: Contours of the Weibull parameters using micro-droplets data for normal use conditions (left panel), and accelerated conditions (right panel)

Using $(m_{11}, m_{12}) = (5, 10)$ and $(m_{21}, m_{22}) = (10, 15)$, three UHC samples are generated with CSPALT at different threshold levels $T_{ij}(i, j = 1, 2)$; see Table 19. For each sample $\mathbb{S}_i(i = 1, 2, 3)$, the MLEs and corresponding 95% ACIs for θ, μ, β, $R_1(t)$, and $H_1(t)$ at $t = 1$ are computed. Since no prior information is available for the Weibull parameters θ and μ from the WOLED datasets,

the hyperparameters c_i and $v_i (i = 1, 2)$ are chosen to be 0.001, representing nearly non-informative improper gamma priors. With $\mathcal{M} = 50{,}000$ total iterations and $\mathcal{Q} = 10{,}000$ burn-in iterations in the MCMC procedure described in Section 4, the Bayesian MCMC point estimates and associated 95% BCIs for θ, μ, β, $R_1(t)$, and $H_1(t)$ are obtained. The initial values for θ, μ, and β in the MCMC algorithm are set to their corresponding frequentist estimates. Table 20 reports the classical and Bayesian point estimates (with their Std.Es) alongside the asymptotic and credible intervals (with their interval widths). Based on the smallest Std.Ers and shortest IWs, Table 20 shows that the Bayesian estimates perform better than those from the frequentist method.

Table 19: Artificial UHC samples using CSPALT from micro-droplets data

Sample	(τ_1, τ_2)	$(T_{11}(r_{11}), T_{12}(r_{12}))$ $(T_{21}(r_{21}), T_{22}(r_{22}))$	Data
$\mathcal{S}1$	(3.3, 2.62)	(3.3(12), 3.5(12))	0.94, 1.08, 1.10, 1.60, 1.92, 2.28, 2.48, 2.60, 2.76, 3.00, 3.22, 3.22
		(2.5(10), 2.7(15))	1.60, 1.80, 1.94, 2.02, 2.18, 2.30, 2.30, 2.30, 2.36, 2.44, 2.50, 2.54, 2.58, 2.60, 2.62
$\mathcal{S}2$	(2.7, 2.6)	(2.3(6), 2.7(8))	0.94, 1.08, 1.10, 1.60, 1.92, 2.28, 2.48, 2.60
		(2.2(5), 2.6(12))	1.60, 1.80, 1.94, 2.02, 2.18, 2.30, 2.30, 2.30, 2.36, 2.44, 2.50, 2.54
$\mathcal{S}3$	(1.92, 2.44)	(1.1(2), 1.5(4))	0.94, 1.08, 1.10, 1.60, 1.92
		(2.1(4), 2.4(9))	1.60, 1.80, 1.94, 2.02, 2.18, 2.30, 2.30, 2.30, 2.36, 2.44

Table 20: Estimates of θ, μ, β, $R_1(t)$, and $H_1(t)$ from micro-droplets data

Sample	Par.	MLE MCMC		95% ACI 95%		
		Est.	Std.E	Low.	Upp.	IW
$\mathcal{S}1$	θ	3.7085	2.3138	0.0000	8.2434	8.2434
		3.7078	0.0197	3.6702	3.7464	0.0761
	μ	0.0153	0.0002	0.0149	0.0157	0.0007
		0.0158	0.0030	0.0107	0.0222	0.0115
	β	2.0298	1.7679	0.0000	5.4948	5.4948
		2.0299	0.0201	1.9906	2.0692	0.0785
	$R_1(t)$	0.9848	0.0002	0.9845	0.9852	0.0007
		0.9843	0.0029	0.9781	0.9894	0.0113
	$H_1(t)$	0.0568	0.0348	0.0000	0.1249	0.1249
		0.0587	0.0111	0.0398	0.0821	0.0424
$\mathcal{S}2$	θ	2.7678	1.5683	0.0000	5.8416	5.8416
		2.7676	0.0202	2.7281	2.8072	0.0791
	μ	0.0257	0.0005	0.0247	0.0267	0.0020

(Continued)

Table 20 (continued)

Sample	Par.	MLE / MCMC		95% ACI / 95%		
		Est.	Std.E	Low.	Upp.	IW
		0.0268	0.0057	0.0169	0.0389	0.0220
	β	2.2236	2.4532	0.0000	7.0318	7.0318
		2.2234	0.0199	2.1842	2.2625	0.0782
	$R_1(t)$	0.9746	0.0005	0.9736	0.9756	0.0020
		0.9735	0.0056	0.9618	0.9832	0.0214
	$H_1(t)$	0.0712	0.0391	0.0000	0.1478	0.1478
		0.0742	0.0158	0.0468	0.1076	0.0608
$\mathcal{S}3$	θ	3.0170	2.2210	0.0000	7.3701	7.3701
		3.0169	0.0202	2.9773	3.0564	0.0791
	μ	0.0186	0.0003	0.0180	0.0192	0.0012
		0.0197	0.0049	0.0115	0.0302	0.0187
	β	2.2919	2.9696	0.0000	8.1122	8.1122
		2.2918	0.0200	2.2522	2.3309	0.0787
	$R_1(t)$	0.9815	0.0003	0.9809	0.9821	0.0012
		0.9805	0.0048	0.9702	0.9885	0.0183
	$H_1(t)$	0.0562	0.0406	0.0000	0.1358	0.1358
		0.0595	0.0147	0.0347	0.0910	0.0563

Contour plots in Fig. 8 assess the existence and uniqueness of the likelihood estimates for θ, μ, and β from Samples $\mathcal{S}_i (i = 1, 2, 3)$. The plots confirm that the estimates are unique and align with the results reported in Tables 19 and 20. We recommend these estimates as initial values for further MCMC analysis. Fig. 9 shows the Gaussian kernel density and trace plots (Sample $\mathcal{S}_1$) of θ, μ, β, $R_1(t)$, and $H_1(t)$. The acquired 40,000 variates show good mixing; specifically, the posteriors of θ and β are roughly symmetric; μ and $H_1(t)$ are positively skewed; $R_1(t)$ is negatively skewed. These results also indicate that the burn-in period effectively removed initialization effects and ensured proper mixing. The statistics of θ, μ, β, $R_1(t)$, and $H_1(t)$ confirm the same findings listed in Table 21 and the same facts shown in Fig. 9.

The industrial relevance lies in showing that by applying the Weibull-based UHC with CSPALT framework, manufacturers can obtain reliable lifetime estimates for LEDs and Micro-droplets under shortened test durations with fewer failures observed, which directly translates to reduced testing costs, faster qualification, and more efficient reliability assessment in practice.

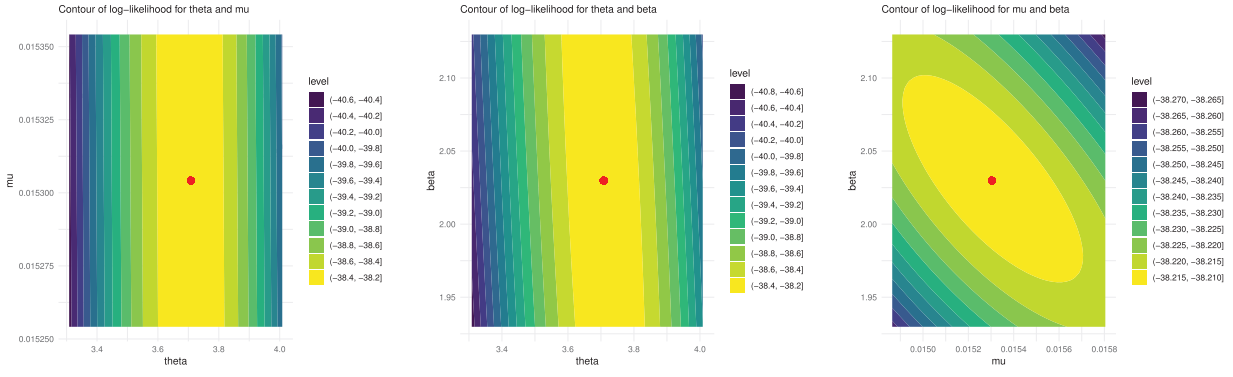

(a) Sample $\mathcal{S}1$

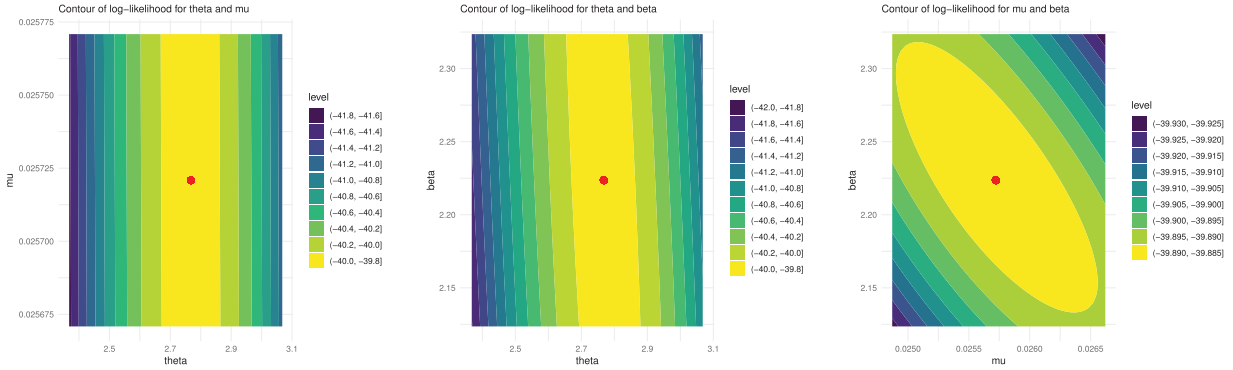

(b) Sample $\mathcal{S}2$

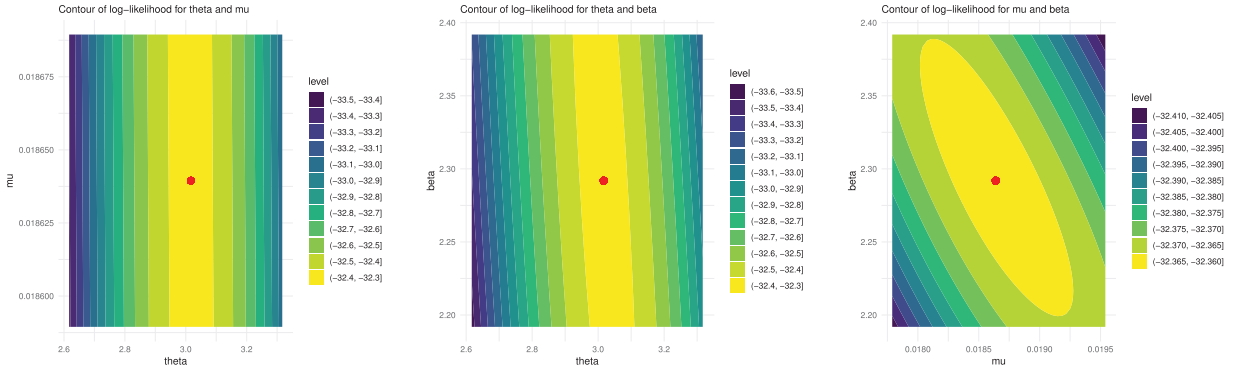

(c) Sample $\mathcal{S}3$

Figure 8: Likelihood contours of θ (left), μ (middle), and β (right) from micro-droplets data: (**a**) Sample $\mathcal{S}1$, (**b**) Sample $\mathcal{S}2$, and (**c**) Sample $\mathcal{S}3$

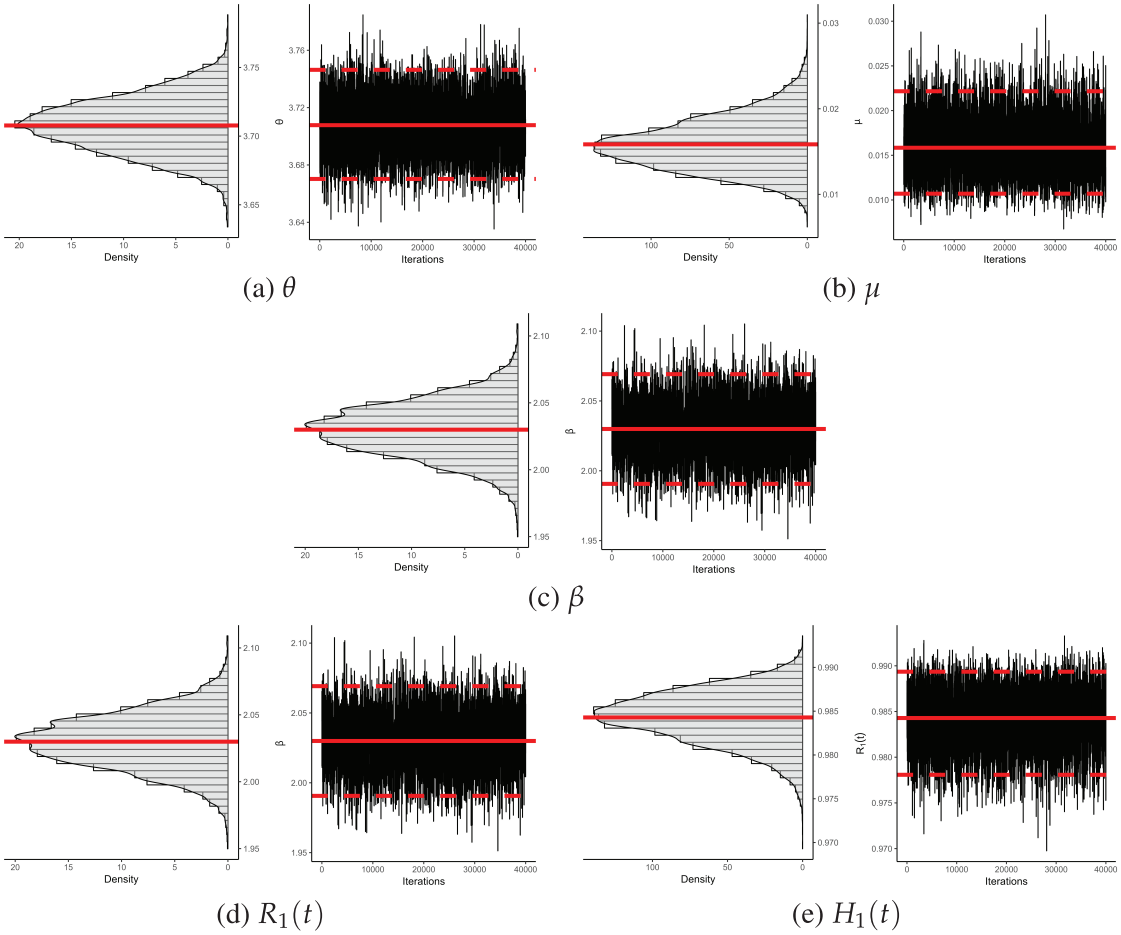

(a) θ (b) μ

(c) β

(d) $R_1(t)$ (e) $H_1(t)$

Figure 9: Density (left) and Trace (right) of θ, μ, β, $R_1(t)$, and $H_1(t)$ from micro-droplets data: (**a**) θ, (**b**) μ, (**c**) β, (**d**) $R_1(t)$, and (**e**) $H_1(t)$

Table 21: Statistics of θ, μ, β, $R_1(t)$, and $H_1(t)$ from micro-droplets data

Sample	Par.	Mean	Q_1	Q_2	Q_3	Mode	SD	Sk.
$\mathcal{S}1$	θ	3.7078	3.7338	3.6942	3.7080	3.7213	0.0197	−0.0101
	μ	0.0158	0.0149	0.0137	0.0157	0.0177	0.0029	0.3691
	β	2.0299	2.0251	2.0163	2.0303	2.0439	0.0201	−0.0378
	$R_1(t)$	0.9843	0.9852	0.9824	0.9845	0.9864	0.0029	−0.3606
	$H_1(t)$	0.0587	0.0558	0.0509	0.0581	0.0657	0.0109	0.3652
$\mathcal{S}2$	θ	2.7676	2.7768	2.7540	2.7674	2.7813	0.0202	0.0125
	μ	0.0268	0.0257	0.0228	0.0264	0.0304	0.0056	0.4019
	β	2.2234	2.2415	2.2102	2.2229	2.2369	0.0199	0.0362
	$R_1(t)$	0.9735	0.9746	0.9701	0.9739	0.9774	0.0055	−0.3847

(Continued)

Table 21 (continued)

Sample	Par.	Mean	Q_1	Q_2	Q_3	Mode	SD	Sk.
	$H_1(t)$	0.0742	0.0714	0.0632	0.0731	0.0841	0.0155	0.3974
$\mathcal{S}3$	θ	3.0169	3.0260	3.0031	3.0167	3.0307	0.0202	0.0009
	μ	0.0197	0.0186	0.0163	0.0193	0.0227	0.0048	0.4775
	β	2.2918	2.3098	2.2785	2.2912	2.3054	0.0200	0.0260
	$R_1(t)$	0.9805	0.9815	0.9776	0.9809	0.9838	0.0047	−0.4623
	$H_1(t)$	0.0595	0.0564	0.0493	0.0583	0.0683	0.0143	0.4745

7 Concluding Remarks

In this study, we integrated constant-stress partially accelerated life testing with a unified hybrid censoring scheme to efficiently collect failure data for highly durable products, thereby significantly reducing experimental duration and costs. The Weibull distribution, recognized for its versatility in modeling diverse failure patterns, was adopted to characterize product lifetimes. The classical and Bayesian estimations of the Weibull distribution were conducted, including the estimation of model parameters and the acceleration factor. A key objective of the life testing experiment is the analysis of reliability metrics. Under normal operating conditions, we examined the estimation of two critical reliability measures, namely the reliability function and the hazard rate function. The maximum likelihood estimators, approximate confidence intervals, Bayes point estimators, and Bayesian credible intervals were all studied and reported. For Bayesian estimation, gamma priors were assigned to the model parameters, while a non-informative prior is used for the acceleration factor. The Markov Chain Monte Carlo sampling procedure, utilizing the Metropolis-Hastings within Gibbs algorithm, is employed to perform the Bayesian analysis. To evaluate the accuracy of the derived estimates and compare the effectiveness of various interval estimation methods, a Monte Carlo simulation study is conducted. Ultimately, two real-world data sets gathered from engineering and clinical sectors are analyzed to demonstrate the practical application of the proposed estimation procedures. Some limitations of the current study include: (1) Assuming Weibull lifetimes, if the true distribution differs, reliability and hazard estimates may be biased. (2) Bayesian inference via Markov Chain Monte Carlo techniques can be computationally demanding for large datasets, limiting scalability, and may be sensitive to prior choices. (3) Simulations and case studies use specific sample sizes and censoring thresholds, so generalizability to other designs warrants further investigation. As future work, it is of interest to extend the current study to investigate the parameter identifiability under the unified hybrid censoring and partially accelerated life tests. Another direction for future research is to extend the Bayesian estimation of the model parameters and the reliability function under normal use conditions by employing alternative loss functions, such as the linear–exponential loss and generalized entropy loss functions.

Acknowledgement: The authors would like to express thank to Princess Nourah bint Abdulrahman University for funding this research work through the Research Group Project, Grant No. (RG-1445-0024).

Funding Statement: The authors extend their appreciation to the Deanship of Scientific Research and Libraries in Princess Nourah bint Abdulrahman University for funding this research work through the Research Group Project, Grant No. (RG-1445-0024).

Author Contributions: Funding acquisition: Ohud A. Alqasem; Methodology: Ohud A. Alqasem and Mazen Nassar; Formal Analysis: Maysaa Elmahi Abd Elwahab and Mazen Nassar; Writing—original draft: Ahmed Elshahhat and Ohud A. Alqasem and Mazen Nassar; Project administration: Ohud A. Alqasem and Maysaa Elmahi Abd Elwahab; Writing—review & editing: Mazen Nassar and Ahmed Elshahhat. Data curation: Ahmed Elshahhat and Mazen Nassar, Software: Ahmed Elshahhat and Ohud A. Alqasem. All authors reviewed the results and approved the final version of the manuscript.

Availability of Data and Materials: Data available within the article.

Ethics Approval: Not applicable.

Conflicts of Interest: The authors declare no conflicts of interest to report regarding the present study.

References

1. Watkins AJ, John AM. On constant stress accelerated life tests terminated by Type II censoring at one of the stress levels. J Stat Plan Inference. 2008;138(3):768–86. doi:10.1016/j.jspi.2007.02.013.
2. Fan TH, Yu CH. Statistical inference on constant stress accelerated life tests under generalized gamma lifetime distributions. Qual Reliab Eng Int. 2013;29(5):631–8. doi:10.1002/qre.1412.
3. El-Din MM, Abu-Youssef SE, Ali NS, El-Raheem AA. Estimation in constant-stress accelerated life tests for extension of the exponential distribution under progressive censoring. Metron. 2016;74(2):253–73. doi:10.1007/s40300-016-0089-4.
4. Abd El-Raheem AM. Optimal plans of constant-stress accelerated life tests for extension of the exponential distribution. J Test Eval. 2019;47(2):1586–605. doi:10.1520/jte20170227.
5. Kumar D, Nassar M, Dey S, Alam FMA. On estimation procedures of constant stress accelerated life test for generalized inverse Lindley distribution. Qual Reliab Eng Int. 2022;38(1):211–28. doi:10.1002/qre.2971.
6. Wu W, Wang BX, Chen J, Miao J, Guan Q. Interval estimation of the two-parameter exponential constant stress accelerated life test model under Type-II censoring. Qual Technol Quantitat Manag. 2023;20(6):751–62. doi:10.1080/16843703.2022.2147688.
7. Mohamed ME, Alqasem OA, Nassar M. Analysis and applications of Nakagami constant-stress model using progressive Type-II censored data. Phys Scr. 2025;100(3):035206. doi:10.1088/1402-4896/adae3d.
8. Tang LC, Sun YS, Goh TN, Ong HL. Analysis of step-stress accelerated-life-test data: a new approach. IEEE Trans Reliab. 1996;45(1):69–74. doi:10.1109/24.488919.
9. Fard N, Li C. Optimal simple step stress accelerated life test design for reliability prediction. J Stat Plan Inference. 2009;139(5):1799–808. doi:10.1016/j.jspi.2008.05.046.
10. Han D, Ng HKT. Comparison between constant-stress and step-stress accelerated life tests under time constraint. Nav Res Logist. 2013;60(7):541–56. doi:10.1002/nav.21551.
11. Amleh MA, Raqab MZ. Inference in simple step-stress accelerated life tests for Type-II censoring Lomax data. J Stat Theory Appl. 2021;20(2):364–79.
12. Kateri M, Nikolov NI. Product of spacings estimation in step-stress accelerated life testing: an alternative to maximum likelihood. IEEE Trans Reliab. 2024;73(3):1433–45. doi:10.1109/tr.2024.3369977.
13. Hassan AS, Assar SM, Zaky AN. Constant-stress partially accelerated life tests for inverted Weibull distribution with multiple censored data. Int J Adv Stat Probab. 2015;3(1):72–82. doi:10.14419/ijasp.v3i1.4418.

14. Nassr SG, Elharoun NM. Inference for exponentiated Weibull distribution under constant stress partially accelerated life tests with multiple censored. Commun Statist Applicat Meth. 2019;26(2):131–48. doi:10.29220/csam.2019.26.2.131.
15. Hassan AS, Nassr SG, Pramanik S, Maiti SS. Estimation in constant stress partially accelerated life tests for Weibull distribution based on censored competing risks data. Ann Data Sci. 2020;7(1):45–62. doi:10.1007/s40745-019-00226-3.
16. Alomani GA, Hassan AS, Al-Omari AI, Almetwally EM. Different estimation techniques and data analysis for constant-partially accelerated life tests for power half-logistic distribution. Sci Rep. 2024;14(1):20865. doi:10.1038/s41598-024-71498-w.
17. Fayomi A, Ahmed AA, AL-Sayed NT, Behairy SM, AL-Fattah Abd, A M, et al. Constant stress-partially accelerated life tests of Vtub-shaped lifetime distribution under progressive type II censoring. Symmetry. 2024;16(9):1251. doi:10.3390/sym16091251.
18. Yao H, Gui W. Inference on exponentiated Rayleigh distribution with constant stress partially accelerated life tests under progressive type-II censoring. J Appl Stat. 2025;52(2):448–76. doi:10.1080/02664763.2024.2373930.
19. El Gazar AM, Ramadan DA, ElGarhy M, El-Desouky BS. Estimation of parameters for inverse power Ailamujia and truncated inverse power Ailamujia distributions based on progressive type-II censoring scheme. Innovat Statist Probab. 2025;1(1):76–87. doi:10.64389/isp.2025.01106.
20. Sirvanci M, Yang G. Estimation of the Weibull parameters under type I censoring. J Am Stat Assoc. 1984;79(385):183–7. doi:10.1080/01621459.1984.10477082.
21. Abdel-Hamid AH, AL-Hussaini EK. Estimation in step-stress accelerated life tests for the exponentiated exponential distribution with type-I censoring. Computat Statist Data Anal. 2009;53(4):1328–38. doi:10.1016/j.csda.2008.11.006.
22. Ramzan Q, Amin M, Faisal M. Bayesian inference for modified weibull distribution under simple step-stress model based on type-I censoring. Qual Reliab Eng Int. 2022;38(2):757–79. doi:10.1002/qre.3011.
23. Epstein B. Truncated life tests in the exponential case. Ann Mathem Statist. 1954;25(3):555–64. doi:10.1214/aoms/1177728723.
24. Childs A, Chandrasekar B, Balakrishnan N, Kundu D. Exact likelihood inference based on Type-I and Type-II hybrid censored samples from the exponential distribution. Ann Instit Statist Mathem. 2003;55(2):319–30. doi:10.1007/bf02530502.
25. Chandrasekar B, Childs A, Balakrishnan N. Exact likelihood inference for the exponential distribution under generalized Type-I and Type-II hybrid censoring. Naval Res Logist. 2004;51(7):994–1004. doi:10.1002/nav.20038.
26. Mahmoud MAW, Ghazal MGM. Estimations from the exponentiated rayleigh distribution based on generalized Type-II hybrid censored data. J Egypt Math Soc. 2017;25(1):71–8. doi:10.1016/j.joems.2016.06.008.
27. Alharthi AS, Almulhim FA. Evaluating the lifetime performance index of the generalised half-logistic population in the generalised Type I hybrid censoring scheme. Alexandria Eng J. 2024;105(7):237–44. doi:10.1016/j.aej.2024.05.094.
28. Balakrishnan N, Rasouli A, Sanjari Farsipour N. Exact likelihood inference based on an unified hybrid censored sample from the exponential distribution. J Stat Comput Simul. 2008;78(5):475–88. doi:10.1080/00949650601158336.
29. Kundu D, Gupta RD. Estimation of $P[Y < X]$ for Weibull distributions. IEEE Trans Reliab. 2006;55(2):270–80.
30. Teimouri M, Hoseini SM, Nadarajah S. Comparison of estimation methods for the Weibull distribution. Statistics. 2013;47(1):93–109. doi:10.1080/02331888.2011.559657.
31. Starling JK, Mastrangelo C, Choe Y. Improving Weibull distribution estimation for generalized Type I censored data using modified SMOTE. Reliab Eng Syst Saf. 2021;211(1):107505. doi:10.1016/j.ress.2021.107505.

32. Ramos PL, Almeida MH, Louzada F, Flores E, Moala FA. Objective Bayesian inference for the Capability index of the Weibull distribution and its generalization. Comput Indust Eng. 2022;167:108012. doi:10.1016/j.cie.2022.108012.
33. Nassar M, Elshahhat A. Estimation procedures and optimal censoring schemes for an improved adaptive progressively type-II censored Weibull distribution. J Appl Stat. 2024;51(9):1664–88. doi:10.1080/02664763.2023.2230536.
34. Bahram K, Belhamiani M, Chaib M, Hamidou B, Slimane A, Bouchouicha B. Fatigue life prediction and crack growth analysis of weld zones in API X60 steel using Weibull distribution and Monte Carlo simulations. Theoret Appl Fract Mech. 2025;138(3):104962. doi:10.1016/j.tafmec.2025.104962.
35. Abouelmagd THM, Al-mualim S, Elgarhy M, Ahmed ZA, Ahmad M. Properties of the four-parameter Weibull distribution and its applications. Pakistan J Statis. 2017;33(6):449–66.
36. Elbatal I, Elgarhy M, Kibria BMG. Alpha power transformed Weibull-G family of distributions: theory and applications. J Stat Theory Appl. 2021;20(2):340–54.
37. Alyami SA, Elbatal I, Alotaibi N, Almetwally EM, Okasha HM, Elgarhy M. Topp-leone modified weibull model: theory and applications to medical and engineering data. Appl Sci. 2022;12(20):10431. doi:10.3390/app122010431.
38. Noori NA, Abdullah KN, khaleel MA. Development and applications of a new hybrid weibull-inverse weibull distribution. Modern J Statist. 2025;1(1):80–103. doi:10.64389/mjs.2025.01112.
39. Lone SA, Panahi H, Shah I. Bayesian prediction interval for a constant-stress partially accelerated life test model under censored data. J Taibah Univ Sci. 2021;15(1):1178–87. doi:10.1080/16583655.2021.2023847.
40. Alrashidi A, Rabie A, Mahmoud AA, Nasr SG, Mustafa MSA, Mutairi AA, et al. Exponentiated gamma constant-stress partially accelerated life tests with unified hybrid censored data: statistical inferences. Alexandria Eng J. 2024;88(5):268–75. doi:10.1016/j.aej.2023.12.066.
41. Rabie A, Abd-Elrahman AM. Statistical inference using partially accelerated life test model for the weibull population mean unified hybrid censored data. Int J Reliab Qual Safety Eng. 2024;31(3):2450014. doi:10.1142/s0218539324500141.
42. Henningsen A, Toomet O. maxLik: a package for maximum likelihood estimation in R. Comput Stat. 2011;26(3):443–58. doi:10.1007/s00180-010-0217-1.
43. Plummer M, Best N, Cowles K, Vines K. CODA: convergence diagnosis and output analysis for MCMC. R News. 2006;6(1):7–11.
44. Zhang JP, Cheng GL, Chen X, Han Y, Zhou TJ, Qiu YJ. Accelerated life test of white OLED based on lognormal distribution. Indian J Pure Appl Phy. 2014;52:671–7.
45. Nassar M, Dey S, Wang L, Elshahhat A. Estimation of Lindley constant-stress model via product of spacing with Type-II censored accelerated life data. Communicat Statist-Simul Computat. 2024;53(1):288–314. doi:10.1080/03610918.2021.2018460.
46. Nassar M, Alotaibi R, Elshahhat A. Reliability analysis at usual operating settings for Weibull Constant-stress model with improved adaptive Type-II progressively censored samples. AIMS Math. 2024;9(7):16931–65. doi:10.3934/math.2024823.
47. Aliabadi AA, Rogak SN, Green SI, Bartlett KH. CFD simulation of human coughs and sneezes: a study in droplet dispersion, heat, and mass transfer. In: ASME 2010 International Mechanical Engineering Congress and Exposition; 2010 Nov 12–18; Vancouver, BC, Canada. p. 1051–60.
48. Asadi S, Panahi H, Swarup C, Lone SA. Inference on adaptive progressive hybrid censored accelerated life test for Gompertz distribution and its evaluation for virus-containing micro droplets data. Alex Eng J. 2022;61(12):10071–84. doi:10.1016/j.aej.2022.02.061.
49. Nassar M, Elshahhat A. Statistical analysis of inverse Weibull constant-stress partially accelerated life tests with adaptive progressively type I censored data. Mathematics. 2023;11(2):370. doi:10.3390/math11020370.